Article:

Aad, G., Aakvaag, E., Abbott, B. et al. (2885 more authors) (2024) Search for a resonance decaying into a scalar particle and a Higgs boson in the final state with two bottom quarks and two photons in proton–proton collisions at √s = 13 TeV with the ATLAS detector. Journal of High Energy Physics, 2024 (11). 47. ISSN 1126-6708

https://doi.org/10.1007/jhep11(2024)047

Published for SISSA by Springer

Received: *April 22, 2024*
Accepted: *September 30, 2024*
Published: *November 7, 2024*

Search for a resonance decaying into a scalar particle and a Higgs boson in the final state with two bottom quarks and two photons in proton–proton collisions at $\sqrt{s} = 13$ TeV with the ATLAS detector

The ATLAS collaboration

E-mail: atlas.publications@cern.ch

Abstract: A search for the resonant production of a heavy scalar X decaying into a Higgs boson and a new lighter scalar S, through the process $X \to S(\to b\bar{b})H(\to\gamma\gamma)$, where the two photons are consistent with the Higgs boson decay, is performed. The search is conducted using an integrated luminosity of 140 fb^{-1} of proton-proton collision data at a centre-of-mass energy of 13 TeV recorded with the ATLAS detector at the Large Hadron Collider. The search is performed over the mass range $170 \leq m_X \leq 1000$ GeV and $15 \leq m_S \leq 500$ GeV. Parameterised neural networks are used to enhance the signal purity and to achieve continuous sensitivity in a domain of the (m_X, m_S) plane. No significant excess above the expected background is found and 95% CL upper limits are set on the cross section times branching ratio, ranging from 39 fb to 0.09 fb. The largest deviation from the background-only expectation occurs for $(m_X, m_S) = (575, 200)$ GeV with a local (global) significance of 3.5 (2.0) standard deviations.

Keywords: Hadron-Hadron Scattering, Beyond Standard Model, Higgs Physics, Hadron-Hadron scattering

ArXiv ePrint: 2404.12915

https://doi.org/10.1007/JHEP11(2024)047

JHEP11(2024)047

Contents

1 Introduction

The properties of the Higgs boson (H) discovered in 2012 [1, 2] by the ATLAS and CMS experiments at the Large Hadron Collider (LHC) are consistent with the Standard Model (SM) predictions [3, 4]. However the current experimental precision does not exclude that H may have a small mixing with additional scalar bosons, and may be part of an extended Higgs sector. Many Beyond the Standard Model (BSM) theories predict such an extended Higgs sector, where one of the physical Higgs boson states could correspond to the spin-0 boson observed with a mass of 125 GeV, while additional scalars remain to be discovered [5].

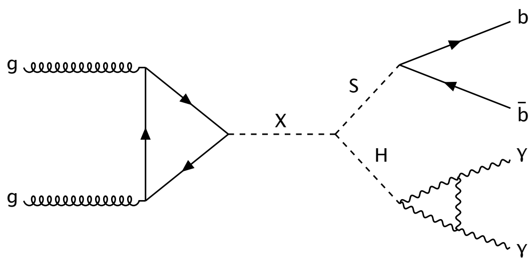

Figure 1. Example of a Feynman diagram showing gluon–gluon fusion production of a scalar X decaying into a scalar S and a Standard Model Higgs boson, which in turn decay into a pair of b-quarks and a pair of photons.

In this paper, the complete proton-proton dataset collected by the ATLAS experiment during Run 2 of the LHC is used to search for two additional scalar bosons X and S. Under the condition $m_X > m_S + m_H$, the decay $X \to SH$ is kinematically allowed. This phenomenology may arise in models where the SM Higgs sector is extended with either a complex singlet [6] or two real singlets [7], and in models such as the complex two-Higgs-doublet model (2HDM) [8], the 2HDM extended by a real scalar singlet [9, 10] or the Next-to-Minimal Supersymmetric Standard Model [11, 12].

The sensitivity of the LHC to the decay $X \to SH$ has been explored in several benchmark scenarios [7, 13, 14]. The decay of the scalar S is model- and mass-dependent. The CMS Collaboration has performed searches for $X \to S(\to b\bar{b})H(\to b\bar{b})$, $X \to S(\to b\bar{b})H(\to \tau\bar{\tau})$ and $X \to S(\to b\bar{b})H(\to \gamma\gamma)$ using Run 2 data [15–17]. In the $X \to S(\to b\bar{b})H(\to \gamma\gamma)$ final state, CMS observed a deviation from the background-only hypothesis with a local (global) significance of 3.8 (2.8) standard deviations at $m_X = 650$ GeV and $m_S = 90$ GeV. ATLAS published results on the search for $X \to S(\to VV)H(\to \tau\bar{\tau})$, where V denotes a W or Z boson [18].

This paper is focused on the search for $X \to S(\to b\bar{b})H(\to \gamma\gamma)$ and uses the same Run 2 dataset already exploited by ATLAS to search for Higgs boson pair production [19]. A di-photon mass peak arises from $H \to \gamma\gamma$, while the two b-tagged jets arise from the $S \to b\bar{b}$ decay, thus leading to a characteristic signal with three resonant mass peaks from $H \to \gamma\gamma$, $S \to b\bar{b}$ and $X \to b\bar{b}\gamma\gamma$. The natural widths of the new bosons are assumed to be much smaller than the experimental resolutions. In the particular scenario where the scalar S has couplings similar to those of the SM Higgs boson, $S \to b\bar{b}$ is the predominant decay for $m_S < 130$ GeV. The Feynman diagram for the main production mode of this process is illustrated in figure 1.

The rate of production for the scalar X, and the decay branching ratios $BR(X \to SH)$ and $BR(S \to b\bar{b})$, are strongly dependent on which model is realised, and on the specific values of the parameters of the extended Higgs sector. Therefore, the results are expressed as 95% confidence level (CL) upper limits on $\sigma(pp \to X) \times BR(X \to SH) \times BR(S \to b\bar{b}) \times BR(H \to \gamma\gamma)$, denoted $\sigma(X \to SH \to b\bar{b}\gamma\gamma)$, rather than on specific models, probing the m_X range between 170 and 1000 GeV and the m_S range between 15 and 500 GeV.

This article is structured as follows. Section 2 briefly introduces the ATLAS detector. Data and simulated event samples are given in section 3. Object definitions are introduced in

JHEP11(2024)047

section 4 while the event selection is described in section 5. The strategy for background estimation is explained in section 6. Section 7 is devoted to the description of the systematic uncertainties. Statistical modelling, validation of the background calculations and results are presented in section 8. Finally the conclusions are given in section 9.

2 ATLAS detector

The ATLAS detector [20] at the LHC covers nearly the entire solid angle around the collision point.[1] It consists of an inner tracking detector surrounded by a thin superconducting solenoid, electromagnetic and hadronic calorimeters, and a muon spectrometer incorporating three large superconducting air-core toroidal magnets.

The inner-detector system (ID) is immersed in a 2 T axial magnetic field and provides charged-particle tracking in the range $|\eta| < 2.5$. The high-granularity silicon pixel detector covers the vertex region and typically provides four measurements per track, the first hit generally being in the insertable B-layer (IBL) installed before Run 2 [21, 22]. It is followed by the SemiConductor Tracker (SCT), which usually provides eight measurements per track. These silicon detectors are complemented by the transition radiation tracker (TRT), which enables radially extended track reconstruction up to $|\eta| = 2.0$. The TRT also provides electron identification information based on the fraction of hits (typically 30 in total) above a higher energy-deposit threshold corresponding to transition radiation.

The calorimeter system covers the pseudorapidity range $|\eta| < 4.9$. Within the region $|\eta| < 3.2$, electromagnetic calorimetry is provided by a lead/liquid-argon (LAr) sampling calorimeter with accordion geometry. It is divided into a barrel section covering $|\eta| < 1.475$ and two endcap sections covering $1.375 < |\eta| < 3.2$. For $|\eta| < 2.5$, it is divided into three layers in depth, which are finely segmented in η and ϕ. An additional thin LAr presampler layer covering $|\eta| < 1.8$ is used to correct for energy loss in material upstream of the calorimeters. Hadronic calorimetry is provided by the steel/scintillator-tile calorimeter, segmented into three barrel structures within $|\eta| < 1.7$, and two copper/LAr hadronic endcap calorimeters. The solid angle coverage is completed with forward copper/LAr and tungsten/LAr calorimeter modules optimised for electromagnetic and hadronic energy measurements respectively.

The muon spectrometer (MS) comprises separate trigger and high-precision tracking chambers measuring the deflection of muons in a magnetic field generated by the superconducting air-core toroidal magnets. The field integral of the toroids ranges between 2.0 and 6.0 T m across most of the detector. Three layers of precision chambers, each consisting of layers of monitored drift tubes, cover the region $|\eta| < 2.7$, complemented by cathode-strip chambers in the forward region, where the background is highest. The muon trigger system covers the range $|\eta| < 2.4$ with resistive-plate chambers in the barrel, and thin-gap chambers in the endcap regions.

[1] ATLAS uses a right-handed coordinate system with its origin at the nominal interaction point (IP) in the centre of the detector and the z-axis along the beam pipe. The x-axis points from the IP to the centre of the LHC ring, and the y-axis points upwards. Polar coordinates (r, ϕ) are used in the transverse plane, ϕ being the azimuthal angle around the z-axis. The pseudorapidity is defined in terms of the polar angle θ as $\eta = -\ln\tan(\theta/2)$ and is equal to the rapidity $y = \frac{1}{2}\ln\left(\frac{E+p_z c}{E-p_z c}\right)$ in the relativistic limit. Angular distance is measured in units of $\Delta R \equiv \sqrt{(\Delta y)^2 + (\Delta\phi)^2}$.

The luminosity is measured mainly by the LUCID–2 [23] detector that records Cherenkov light produced in the quartz windows of photomultipliers located close to the beampipe.

Events are selected by the first-level trigger system implemented in custom hardware, followed by selections made by algorithms implemented in software in the high-level trigger [24]. The first-level trigger accepts events from the 40 MHz bunch crossings at a rate below 100 kHz, which the high-level trigger further reduces in order to record complete events to disk at about 1 kHz.

A software suite [25] is used in data simulation, in the reconstruction and analysis of real and simulated data, in detector operations, and in the trigger and data acquisition systems of the experiment.

3 Data and simulated event samples

The data used in this search were collected by the ATLAS experiment between 2015 and 2018, from proton-proton collisions at $\sqrt{s} = 13$ TeV at the LHC. After data quality requirements [26], this corresponds to an integrated luminosity of 140 fb^{-1}. The uncertainty in the combined 2015–2018 integrated luminosity is 0.83% [27], obtained using the LUCID-2 detector [23] for primary luminosity measurements, complemented by measurements using the inner detector and calorimeters.

Events are recorded using diphoton triggers that require two reconstructed photon candidates with minimum transverse energies of 35 GeV and 25 GeV [28]. The triggers used in 2015 and 2016 require both the photons to satisfy the *Loose* photon identification criterion defined in ref. [29], while the *Medium* criterion [29] is used for 2017–2018 to cope with the increased pp interaction rate.

The Monte Carlo (MC) simulated event samples used in the analysis are listed in table 1, along with the generator used in the simulation, the parton distribution function (PDF) set, the showering model and the set of tuned parameters (tune). The $X \to SH$ signal process is simulated at leading-order (LO) in QCD with Pythia 8.2 [30]. The Higgs boson is forced to decay into two photons, while the scalar S is forced to decay into two b-quarks. The X and S scalar decays are generated in the narrow-width approximation. A total of 161 signal mass points are generated in the range $170 \leq m_X \leq 1000$ GeV and $15 \leq m_S \leq 500$ GeV.

The backgrounds can be divided into three categories. The largest background category consists of events with two photon candidates featuring a smoothly falling, non-resonant diphoton mass spectrum. This population arises from processes with two prompt photons or from jet processes where one or both the photon candidates are misidentified jets via instrumental effects. The processes $Z(\to q\bar{q})\gamma\gamma$ and $t\bar{t}\gamma\gamma$ are also included in this category. All these backgrounds together are referred to as 'non-resonant diphoton background', the category is denoted $\gamma\gamma$+jets for short but does include γ+jets and dijet processes. Due to the significant contribution from instrumental background in the $\gamma\gamma$+jets category, its normalisation is constrained with data using dedicated control regions detailed in section 6.1.

The processes $\gamma\gamma$+jets and $Z(\to q\bar{q})\gamma\gamma$, with two real photons, are simulated with Sherpa 2.2.4 and Sherpa 2.2.11 [33] respectively. Matrix elements at next-to-leading-order (NLO) in QCD for up to one parton and at LO for up to three partons are calculated with the Comix [52] and OpenLoops [53–55] libraries. An alternative $\gamma\gamma$+jets MC sample

JHEP11(2024)047

Process	Generator	PDF set	Showering	Tune
$X \to SH$	Pythia 8.2 [30]	NNPDF2.3lo [31]	Pythia 8.2 [30]	A14 [32]
$\gamma\gamma$+jets	Sherpa 2.2.4 [33]	NNPDF3.0nnlo [34]	–	–
$t\bar{t}\gamma\gamma$	MadGraph5_aMC@NLO [35]	NNPDF2.3lo	Pythia 8.2	A14
$Z(\to q\bar{q})\gamma\gamma$	Sherpa 2.2.11 [33]	NNPDF3.0nnlo	–	–
ggF H	Nnlops [36–38] [39, 40]	PDF4LHC15 [41]	Pythia 8.2	AZNLO [42]
VBF H	Powheg Box v2 [43–46]	PDF4LHC15	Pythia 8.2	AZNLO
WH	Powheg Box v2 [47, 48]	PDF4LHC15	Pythia 8.2	AZNLO
$qq \to ZH$	Powheg Box v2 [47, 48]	PDF4LHC15	Pythia 8.2	AZNLO
$gg \to ZH$	Powheg Box v2 [47, 48]	PDF4LHC15	Pythia 8.2	AZNLO
$t\bar{t}H$	Powheg Box v2 [49]	NNPDF3.0nlo	Pythia 8.2	A14
$b\bar{b}H$	Powheg Box v2 [37]	NNPDF3.0nlo	Pythia 8.2	A14
tHq	MadGraph5_aMC@NLO	NNPDF3.0nlo	Pythia 8.2	A14
tHW	MadGraph5_aMC@NLO	NNPDF3.0nlo	Pythia 8.2	A14
ggF HH	Powheg Box v2 +FT [46, 50, 51]	PDFLHC	Pythia 8.2	A14
VBF HH	MadGraph5_aMC@NLO	NNPDF3.0nlo	Pythia 8.2	A14

Table 1. Summary of the main signal and background samples, split by production mode: signal samples, continuum background samples, single Higgs boson processes and Higgs-boson pair production samples. The generator used in the simulation, the PDF set, the showering model and the set of tuned parameters are also provided.

generated with MadGraph5_aMC@NLO [35] including production of up to two jets at NLO is considered for evaluation of systematic uncertainties. The $t\bar{t}\gamma\gamma$ process is generated with MadGraph5_aMC@NLO.

The second largest background category consists of processes with photons from a single Higgs boson decay, this includes processes where the Higgs boson may be produced in association with other particles. This includes single Higgs boson production via gluon–gluon fusion (ggF), vector-boson fusion (VBF), WH, ZH ($qq \to ZH$ and $gg \to ZH$), $t\bar{t}H$, $b\bar{b}H$, tHq and tHW. The cross sections of the single Higgs boson processes are set to the most precise available theoretical values [56].

The last background category consists of Standard Model Higgs boson pair production (HH) processes via ggF and VBF. The ggF Higgs boson pair production cross section is calculated at next-to-next-to-leading-order (NNLO) accuracy including finite top-quark mass effects [57–60]. The cross section for Higgs boson pair production via VBF is calculated at next-to-next-to-next-to-leading-order (N^{3}LO) [57]. The analysis assumes a branching ratio of 0.227% for the Higgs boson decay into two photons and a branching ratio of 58.2% for the Higgs boson decay into two b-quarks [56, 61].

The samples use EvtGen [62] for the modelling of b- and c-hadron decays. A full simulation of the ATLAS detector [63] based on Geant4 [64] is used to reproduce the detector response for single Higgs boson processes. The samples for signal, non-resonant photon production and Standard Model Higgs boson pair production are processed with the fast simulation AtlFastII [65] which employs Geant4 except for a parameterisation of the calorimeter response.

JHEP11(2024)047

Varying numbers of minimum-bias interactions produced with PYTHIA 8.186 [66] using the NNPDF2.3LO PDF set with the A3 tune [67] are overlaid on the hard-scattering event of all samples to simulate the effect of multiple pp interactions (pile-up) in the same or nearby bunch crossings. The events are reweighted as a function of the number of interactions per bunch crossing to match the distribution in data.

4 Object definitions

Events are required to have at least one reconstructed collision vertex, defined as a vertex associated with at least two tracks with transverse momentum (p_{T}) larger than 0.5 GeV. The primary vertex is selected from the reconstructed collision vertices using a neural network algorithm [68] based on extrapolated photon trajectories and the tracks associated with each candidate vertex.

Photons are reconstructed from topologically connected clusters [29] of energy deposits in the electromagnetic calorimeter in the region $|\eta| < 2.37$, excluding the transition region between the barrel and endcap calorimeters $1.37 < |\eta| < 1.52$. Photon candidates are classified as converted or unconverted based on whether or not they can be associated to conversion vertices or tracks consistent with photon conversions.

The calibration of the photon energy is based on a multivariate regression algorithm trained with MC samples, where the simulated distributions of the input variables are corrected with data-driven techniques. The calibrated energy is brought to the absolute scale by applying scale factors derived from $Z \to e^+e^-$ events [29]. The photon direction is reconstructed using the longitudinal development of the shower in the calorimeters constrained to the luminous region of the proton-beam collisions. In the case of converted photons the information about the position of the conversion vertex and the tracks associated with conversion is also used.

Photon identification is based on the lateral shower profile of the energy deposits in the first and second electromagnetic calorimeter layers and on the energy leakage fraction into the hadronic calorimeter [29]. It reduces the misidentification of hadronic jets containing large neutral components, primarily neutral pions, which decay into a pair of highly collimated photons. Identification criteria are tuned for converted and unconverted photons separately, and the *Tight* criteria defined in ref. [29] are applied.

To improve rejection of misidentified photons, two isolation variables are defined to quantify the amount of activity around a photon. Calorimeter-based isolation $E_{\mathrm{T}}^{\mathrm{iso}}$ is defined as the sum of the transverse energy of topological clusters within a cone of size $\Delta R = \sqrt{\Delta\eta^2 + \Delta\phi^2} = 0.2$ around the photon, after first correcting for the energy of the photon candidate itself and for an average expected pile-up contribution. Track-based isolation $p_{\mathrm{T}}^{\mathrm{iso}}$ is defined as the scalar sum of the transverse momenta of all tracks with $p_{\mathrm{T}} > 1$ GeV originating from the primary vertex and within a cone of size $\Delta R = 0.2$ around the photon. To be considered isolated a photon must have $E_{\mathrm{T}}^{\mathrm{iso}}/E_{\mathrm{T}} < 0.065$ and $p_{\mathrm{T}}^{\mathrm{iso}}/E_{\mathrm{T}} < 0.05$. For isolated photons with transverse energies between 30 GeV and 250 GeV, the identification efficiency ranges from 84% to 98% [29].

Electrons are reconstructed from energy deposits measured in the electromagnetic calorimeter that are matched to ID tracks [29]. They are required to be in the region $|\eta| <$

2.37, excluding the transition region between the barrel and endcap calorimeters $1.37 < |\eta| < 1.52$, and to have $p_T > 10$ GeV. Electrons are required to satisfy a *Medium* identification criterion based on the shower shape, track-cluster matching and TRT information in a likelihood-based algorithm [29]. Muons are reconstructed from high-quality tracks found in the MS [69]. A matching of the MS tracks to ID tracks is required in the region $|\eta| < 2.5$. Muons are required to have $|\eta| < 2.7$ and $p_T > 10$ GeV and to satisfy a *Medium* identification criterion [70]. Electrons and muons are both matched to the primary vertex via requirements on the longitudinal and transverse impact parameters on the tracks, $|z_0|$ and $|d_0|$, respectively. These requirements are $|z_0| \sin\theta < 0.5$ mm, and $|d_0|/\sigma_{d_0} < 5$ (3) for electrons (muons).

Reconstructed jets are based on particle-flow objects built from noise-suppressed positive-energy topological clusters in the calorimeter and reconstructed tracks [71]. The anti-k_t algorithm [72, 73] with radius parameter $R = 0.4$ is used. The jet energy is calibrated by applying several simulation-based corrections and techniques correcting for differences between simulation and data [74]. Jets are required to have rapidity $|y| < 4.4$ and $p_T > 25$ GeV. To suppress jets produced in pile-up interactions, each jet within the tracking acceptance of $|\eta| < 2.4$ and with $p_T < 60$ GeV is required to satisfy the *Tight* jet-vertex tagger [75] criteria used to identify jets from the selected primary vertex.

The flavour of jets is determined using a deep-learning neural network, DL1r [76]. The DL1r b-tagging is based on distinctive features of b-hadron decays in terms of the impact parameters of the tracks and the displaced vertices reconstructed in the ID. The inputs of the DL1r network also include discriminating variables constructed by a recurrent neural network (RNNIP) [77], which exploits the spatial and kinematic correlations between tracks originating from the same b-hadron. For each jet, DL1r gives three different probabilities p_b-, p_c- and p_{light} for the jet to originate from a b, c or light quark respectively. The three probabilities are combined to define the final discriminant. The DL1r algorithm is optimised to maximise performance on particle-flow jets and extends the algorithm performance to very high jet p_T. Only central jets with $|\eta| < 2.5$ are considered for flavour tagging. Working points are defined by single requirement values on the DL1r discriminant output distribution, and can be chosen to provide a specific b-jet efficiency for an inclusive $t\bar{t}$ MC sample. The analysis makes use of the DL1r working point with a 77% efficiency to select jets containing b-hadrons in simulated $t\bar{t}$ events. For this working point the misidentification rate is 1/130 for light-flavour jets and 1/4.9 for charm jets. Scale factors are applied to correct for differences in b-tagging efficiency between data and simulation. The scale factors are measured as a function of the jet p_T using a likelihood-based method in a sample enriched in $t\bar{t}$ events [78].

Scale factors are applied to correct for differences in b-tagging efficiency between data and simulation. The scale factors for jets originating from a b quark are measured as a function of the jet p_T using a likelihood-based method in a sample enriched in $t\bar{t}$ events [78]. The scale factors for jets originating from a c quark are measured in $t\bar{t}$ events containing a $W \to cs$ decay [79]. For light flavour jets, the scale factors are derived using Z+jets events [80].

The energy of b-tagged jets is corrected for the possible contribution of muons from semileptonic b-hadron decays. Additionally, the undetected energy of neutrinos and out-of-cone effects are corrected for with scale factors derived as a function of the b-jet p_T from a $t\bar{t}$ MC sample. The two corrections together improve the resolution of the invariant mass of

JHEP11(2024)047

the two jets with the highest b-tagging discriminant by about 20%. This procedure closely follows that in ref. [81].

Overlap removal procedures are applied to avoid using the same detector signals to reconstruct multiple objects. In this analysis priority is given to photons, by removing jets, electrons and muons within $\Delta R < 0.4$ of a selected photon. Next, jets within $\Delta R < 0.2$ of electrons are removed. Finally, electrons and muons within $\Delta R < 0.4$ of any remaining jet are removed.

5 Analysis strategy

A wide range of masses is considered for the scalars X and S, leading to significantly varying event kinematics at different hypothetical values of m_X and m_S. When $m_X \gg m_S + m_H$, the scalar S can become so boosted that its decay products, two b-quarks, become very collimated and are reconstructed within the same $R = 0.4$ jet. For smaller values of $m_X - (m_S + m_H)$, two separate b-tagged jets are reconstructed. Therefore two mutually exclusive regions are defined with either one or two b-tagged jets, referred to as the 1 b-tagged and 2 b-tagged regions, and respectively dedicated to the boosted and non-boosted scenarios. A preselection, common to both regions, is introduced below. A final discriminating variable is then defined for each signal hypothesis using parameterised neural networks. The final experimental constraint on the signal is obtained from a signal-plus-background fit to the distribution of the discriminating variable in data. In the special case where m_S =125 GeV, this analysis strategy can be compared with an alternative strategy similar to that applied in the ATLAS search for $HH \to b\bar{b}\gamma\gamma$ [19], and it was found that for any given signal point the difference between estimated upper limits on $\sigma(X \to SH \to b\bar{b}\gamma\gamma)$ is small.

5.1 Event preselection

Events are selected using diphoton triggers described in section 3. Beyond the trigger requirements, events are selected if:

- At least two photons satisfy the requirements in section 4.
- The invariant mass of the two leading photons satisfies $105 < m_{\gamma\gamma} < 160$ GeV.
- The leading photon has $p_{\mathrm{T}} > 0.35 m_{\gamma\gamma}$ and the subleading photon has $p_{\mathrm{T}} > 0.25 m_{\gamma\gamma}$.
- No electrons or muons, as defined in section 4, are present.
- The number of central ($|\eta| < 2.5$) jets is at least two and no more than five. This reduces the $t\bar{t}H$ background where top quarks decay hadronically.
- There is exactly one or two b-tagged jet at the 77% working point. Events with more than two b-tagged jets are removed to ensure orthogonality with the $b\bar{b}b\bar{b}$ final state from the same signal.

5.2 Signal region definitions

The number of b-tagged jets is used to categorise events in two regions, requiring 1 or 2 b-tagged jets. The signal events contain the characteristic $H \to \gamma\gamma$ decay with the $m_{\gamma\gamma}$ distribution peaking around the Higgs boson mass at $\sim$125 GeV. Therefore, two mutually exclusive signal regions (SR) dedicated respectively to the boosted and non-boosted scenarios are defined requiring $120 < m_{\gamma\gamma} < 130$ GeV. The shape of the final signal-to-background discriminant, defined in section 5.3 for each signal hypothesis, and obtained in the signal region, is used for the final statistical test of the signal-plus-background and background only hypothesis.

Events with $m_{\gamma\gamma}$ outside the [120, 130] GeV interval are instead used to construct the sideband control regions for background estimation as described in section 6. The 2 b-tagged and 1 b-tagged sideband regions (SB) are found to contain about 85% of $\gamma\gamma$+jets with two real photons and are expected to contain less than 0.1% of Higgs boson processes.

The fraction of signal events with two resolved b-tagged jets is below 50% if $m_S/m_X < 0.09$, as derived from simulations. The 1 b-tagged signal region is thus used to analyse signal points for which $m_S/m_X \lesssim 0.09$ and, conversely, the 2 b-tagged selection is used to analyse signal points for which $m_S/m_X \gtrsim 0.09$.

5.3 Final signal-to-background discriminant

Multivariate discriminants are used to separate signal from background events in the signal regions. Two distinct parameterised neural networks (PNNs) [82] are trained with events in the 2 b-tagged and the 1 b-tagged signal and sideband regions. PNNs take as input a vector of event characteristics $\bar{x}$ and a vector of phase space parameters $\bar{\theta}$ and yield a response function that is parameterised in $\bar{\theta}$. The parameterisation provides a unique discriminant for each signal hypothesis, separating the targeted signal events from background events. Therefore, for each value of $\bar{\theta} = (m_S, m_X)$, the PNN($\bar{\theta}$) is effectively a different observable. The PNNs provide sensitivity over the considered mass range and allow interpolation to values of $\bar{\theta}$ not explicitly included in the training. In the 2 b-tagged signal region the PNN is parameterised in the plane of the two particle masses $\bar{\theta} = (m_S, m_X)$, and as a function of $\bar{\theta} = (m_X)$ in the 1 b-tagged region.

The decay chain $X \to S(\to b\bar{b})H(\to\gamma\gamma)$ and the masses m_S and m_X are encoded in the invariant mass of the final state particles, thus the most effective features to train the PNNs are the invariant masses of the final state photons and b-tagged jets.

For the 2 b-tagged signal region the input features are $\bar{x} = (m_{bb}, m^*_{bb\gamma\gamma})$ where $m^*_{bb\gamma\gamma} = m_{bb\gamma\gamma} - (m_{\gamma\gamma} - 125\text{ GeV})$. The replacement of $m_{\gamma\gamma}$ by the Higgs boson mass of 125 GeV allows to remove correlations between the PNN score and $m_{\gamma\gamma}$, allowing to create sideband regions for background normalisation as described in section 6.1. For the 1 b-tagged signal region the input variables are $\bar{x} = (p_{\mathrm{T}}^b, m^*_{b\gamma\gamma})$ where p_{T}^b is the p_{T} of the b-tagged jet, and $m^*_{b\gamma\gamma}$ is derived from the invariant mass $m_{b\gamma\gamma}$ of the only available b-tagged jet and the two photons as $m^*_{b\gamma\gamma} = m_{b\gamma\gamma} - (m_{\gamma\gamma} - 125\text{ GeV})$. Additional variables were considered in the training but did not bring significant improvements and were therefore disregarded. The usage of the variables m_{bb} and $m^*_{bb\gamma\gamma}$ alone allows for the signal interpolation applied in the 2 b-tagged signal region and described in section 5.4.

JHEP11(2024)047

The PNNs are trained using Keras [83] with the Tensorflow [84] backend. The training is performed using 69 simulated signal samples chosen from the entire investigated mass grid, as well as the largest background processes: non-resonant diphoton+jets, $t\bar{t}H$, ZH and ggF H. In the 1 b-tagged signal region the VBF H, and Higgs boson pair production processes are also considered for training. As the vector of parameters $\bar{\theta}$ is not meaningful for the background samples, each background event has $\bar{\theta}$ values assigned at random from the distribution of values in the signal samples during training.

After the signal region selections, most events arise from the $\gamma\gamma$ + jets background category, leading to very unbalanced training classes, which makes it difficult for the PNNs to differentiate between signal and background. The imbalance is reduced by giving a unit weight to all MC events used in the training. The effect of using a unit event weight on the shape of the input features $\bar{x}$ is found to be negligible.

The PNN internal architectures are optimised using KerasTuner [83], which chooses the hyper-parameters maximizing the Area-Under-Curve calculated on an evaluation set and using Bayesian Optimisation [85]. The class weight defined as $w_{\mathrm{c}} = 0.5 n_{\mathrm{tot}}/n_{\mathrm{c}}$ is used, where c is either signal or background, n_{c} is the number of events in the given class and n_{tot} is the total number of events. Furthermore, given the number n_s (n_b) of signal (background) events, an initial bias of $\log(n_s/n_b)$ is applied to the last layer of the PNN.

The PNNs use binary cross entropy as the loss function and stochastic gradient-based optimisation using the Adam algorithm [86]. All hidden layers have a standard dense training layer using a rectified linear unit activation function and each has a dropout layer with a dropout rate between 2% and 20%. The output layers have a single node and use a sigmoid activation function. The PNN used in the 2 b-tagged signal region is trained with signal samples with $m_X \geq 170$ GeV and $m_S \geq 30$ GeV. For the 1 b-tagged signal region, only signal points where S has enough boost are used, this includes eleven points with 15 $\leq m_S$ $\leq$70 GeV. The PNN of the 2 b-tagged signal region has four hidden layers with 85, 49, 45 and 81 nodes. The PNN of the 1 b-tagged signal region has three hidden layers with 101, 29 and 101 nodes. After training, the PNN output shape is compared between data and MC in dedicated sideband regions to validate the modelling of the PNN distribution. The results of these comparisons are covered in section 8.2.

5.4 Signal interpolation

To set continuous limits in the (m_X, m_S) plane, it is desirable to set limits on intermediate signal models where no sample is simulated. In order to constrain an intermediate signal point defined by (m_X^{int}, m_S^{int}), the shape of the PNN output is interpolated from a nearby reference signal sample simulated with low statistical uncertainty and referred to as (m_X^{ref}, m_S^{ref}). The distributions of the input features for (m_X^{int}, m_S^{int}) are derived from the reference sample in two steps: first a rescaling step that takes into account the different masses at the reference and intermediate points, and second a reweighting step that takes different mass resolutions at different mass points into account. The interpolated input features are then used as input to the PNN to obtain the PNN(θ) distribution for the interpolated signal.

For each selected event in the reference sample, the four-vectors of H, S and X are measured using the selected b-jets and photons. The four-vectors of H and S are recomputed in the rest frame of X using a Lorentz transformation defined by the four-vector of X. In absence of any experimental effects, the four-vectors of H and S in the X rest frame would be set to ideal values defined by the kinematics of the $X \to SH$ two-body decay and the specific values of m_X and m_S. In practice, the rest frame quantities are distributions around their ideal values, while the shape of the distributions are determined by experimental effects. The kinematics at the intermediate point ($m_X^{\rm int}$, $m_S^{\rm int}$) are emulated from ($m_X^{\rm ref}$, $m_S^{\rm ref}$) by rescaling the rest frame four-vectors of H and S so that they are distributed around their new ideal theoretical values at ($m_X^{\rm int}$, $m_S^{\rm int}$), and events of the reference sample are weighted to reproduce the expected experimental resolution at the intermediate mass.

The resolution effects are much larger for jets than for photons; therefore, the resolution weighting only considers the m_{bb} resolution. The m_{bb} resolution is measured for the simulated points and modelled with a Bukin probability [87]. Each parameter of the Bukin probability becomes a 2D map in the (m_X, m_S) plane. The values of the Bukin parameters can then be interpolated to any mass point ($m_X^{\rm int}$, $m_S^{\rm int}$) using Delaunay triangulation [88]. The final distribution of PNN($m_X^{\rm int}$, $m_S^{\rm int}$) is obtained by feeding the values of m_{bb} and $m^*_{bb\gamma\gamma}$ to the PNN, after four-vector rescaling and resolution weighting. This technique works well at high momenta where the change in resolution effects between nearby simulated points is small. For this reason the interpolation is only applied in parts of the 2 b-tagged signal region, defined by m_X >300 GeV and m_S >70 GeV.

The quality of the PNN shape interpolation is evaluated by studying its impact on the expected upper limits on $\sigma(X \to SH \to b\bar{b}\gamma\gamma)$. The upper limits obtained with the PNN output shape from simulated signal events are compared with those obtained with the interpolated PNN output shape. In the domain where the interpolation is applied the expected limits on $\sigma(X \to SH \to b\bar{b}\gamma\gamma)$ change by less than 5% for m_S ≥100 GeV when replacing the actual PNN output shape with the interpolated one.

For lower masses (below m_S =70 GeV) fast changes in resolution mean that the limits obtained from interpolated PNN shapes can differ by more than 10% from those obtained with the actual PNN shape. For this reason the interpolation procedure is not applied at low masses or in the 1 b-tagged region. Instead a much finer grid of simulated signal samples in the (m_X, m_S) plane is used. The required granularity is studied by performing injection tests and checking the sensitivity of one PNN at a given $\bar{\theta}$ to neighbouring signal samples generated at a different (m_X, m_S) point. The grid spacing is chosen small enough so that a signal excess at one simulated grid point would also appear in the PNN output of at least one nearby simulated signal sample.

6 Background estimation

The final interpretation in terms of a search for a possible $X \to S(\to b\bar{b})H(\to\gamma\gamma)$ signal requires the ability to predict for each background process the number of events in the signal region, and the shape of the PNN output. In the following sections several methods are employed: a data-driven technique to study the composition of the non-resonant diphoton background category in terms of events with zero, one or two misidentified photons, a data-driven method to normalise the non-resonant diphoton background category, and finally simulations to evaluate contributions from irreducible backgrounds.

6.1 Non-resonant diphoton background

The largest background category is the non-resonant $\gamma\gamma$+jets background, which includes instrumental components such as γ+jets and dijets where jets are misidentified as photons. Other contributions to this category are the $t\bar{t}\gamma\gamma$ process which represents less than 2% (0.5%) of the background in the 2 b-tagged (1 b-tagged) signal region, and the $Z(\to q\bar{q})\gamma\gamma$ process, which represents less than 1% (0.3%) in the 2 b-tagged (1 b-tagged) region. These last two processes are estimated directly from simulation.

The fractions of $\gamma\gamma$+jets events with zero, one or two misidentified photons and their associated systematic uncertainties are determined by the double two-dimensional sideband method, a data-driven technique which relies on several photon identification criteria, already employed in the search for Higgs boson pair production in the $b\bar{b}\gamma\gamma$ final state [19], the method is described in ref. [89] and references therein. The fractions of misidentified photon backgrounds are derived individually in the 1 and 2 b-tagged regions. The fraction of events with two real photons is found to be 87% in the 1 b-tagged region and 84% in the 2 b-tagged region. The data-driven method is also used later to derive the $m_{bb\gamma\gamma}$, $m_{\gamma\gamma}$, m_{bb} and PNN distributions for the different components with true or misidentified photons. These distributions are compared in the sideband regions with the data and the Sherpa $\gamma\gamma$+jets MC sample. No large difference is found between the shapes of the components, indicating that it is possible to directly build high-statistics templates from Sherpa samples without adding contributions from misidentified photons.

Based on these studies, the zero, one or two misidentified photon components of the $\gamma\gamma$+jets background category are modelled directly with the Sherpa $\gamma\gamma$+jets MC sample, with appropriate systematic uncertainties described in section 7. The normalisation of the Sherpa $\gamma\gamma$+jets MC sample is fitted to the data in the sideband and signal regions according to the statistical model described in section 8.1, the fit effectively rescales the Sherpa $\gamma\gamma$+jets MC sample to the sum of the zero, one and two misidentified photon components of the non-resonant diphoton background in data. The rescaling of the Sherpa $\gamma\gamma$+jets MC sample therefore reflects both misidentified photon contributions and higher order processes present in data but not in the simulation. Several systematic uncertainties can affect the ratio of the $\gamma\gamma$+jets background in the signal region over the corresponding sideband as detailed in section 7. In a background-only fit where only the data in the sidebands are considered, this procedure scales the Sherpa $\gamma\gamma$+jets MC sample by a factor 1.03 ± 0.01 in the 1 b-tagged region and a factor 1.26 ± 0.03 in the 2 b-tagged region.

The shape of the PNN output for the non-resonant diphoton category is studied in the sideband regions in both data and simulation, and in the signal regions with simulation. It is observed that the shapes of the PNN output for the zero, one or two misidentified photon components are well reproduced by the Sherpa $\gamma\gamma$+jets MC sample. In the Sherpa $\gamma\gamma$+jets simulation the input variables to the PNN are observed to be consistent within statistical uncertainties between the signal regions and two narrow sidebands defined by $m_{\gamma\gamma} \in$ [115,120] $\cup$ [130,135] GeV. Finally the modelling of the PNN output by simulation is validated in the full sideband control regions, by comparing the predicted PNN distributions from Sherpa $\gamma\gamma$+jets simulations, with the observed PNN distributions in data. Theoretical and experimental systematic uncertainties in the PNN output shapes for the $\gamma\gamma$+jets background category are considered in section 7.

JHEP11(2024)047

6.2 Higgs boson processes

This category of background consists of all processes that contain single Higgs boson production via ggF or VBF, WH, ZH ($qq \to ZH$ and $gg \to ZH$), $t\bar{t}H$, $b\bar{b}H$, tHq and tHW. Higgs boson pair production via ggF and VBF is also included in this category. Following the strategy in ref. [19], the normalisation and shape of these processes are obtained from simulated MC samples generated at NLO, and normalised using state-of-the-art theoretical cross sections [56]. Several systematic uncertainties are assigned to these processes as discussed in section 7.

7 Systematic uncertainties

Three categories of systematic uncertainties are considered. Experimental systematic uncertainties account for possible differences between the performance of the detector in simulation and in data, they are applied to all quantities derived from simulation and are described in section 7.1. Theoretical systematic uncertainties arise where theoretical inputs are used, such as cross sections, or where effects on shapes from higher-order corrections should be considered, this is described in section 7.2. The $\gamma\gamma$+jets background is derived from a combination of MC simulation and a data-driven technique, and the related sytematic uncertainties are detailed in section 7.3.

7.1 Experimental systematic uncertainties

Experimental systematic uncertainties affect selection efficiencies and PNN shapes for all Higgs boson processes and the $X \to S(\to b\bar{b})H(\to\gamma\gamma)$ signal. The effect of experimental systematic uncertainties is also propagated to the PNN shape of the $\gamma\gamma$+jets background. The experimental systematic uncertainties are categorised into four groups, in order of decreasing impact on the expected upper limits on $\sigma(X \to SH \to b\bar{b}\gamma\gamma)$: flavour tagging, photons, jets and pile-up. The limits on $\sigma(X \to SH \to b\bar{b}\gamma\gamma)$ are compared with and without experimental systematic uncertainties. For m_X above $\sim$400 GeV the effect of experimental systematic uncertainties on the limits is less than 1% but grows to 2%–20% at lower m_X values.

Flavour tagging uncertainties [78–80] are the leading source of experimental uncertainties in this search. They include the uncertainties in the efficiency to b-tag a jet containing a b-hadron, and the probability to b-tag a jet containing a c-hadron or a light-flavour jet by mistake. The combined effect of all flavour tagging uncertainties is the largest in the 2 b-tagged signal region with a 5% uncertainty in the signal efficiency for models with low m_S and decreasing to 2% at high m_S. In the 1 b-tagged signal region that uncertainty remains in the range 0.5%–1.5%. The corresponding uncertainty in the predicted number of single and double Higgs boson processes is about 3%. Once incorporated into the fit and taking into account the effect on both the yields and the PNN shapes of signal and backgrounds, flavour tagging uncertainties impact the upper limits by about 6%.

The category of photon-related uncertainties includes uncertainties from efficiencies of the photon triggers, photon identification and isolation, and uncertainties in the photon energy resolution and scale. These are computed in data using data-driven techniques [28, 29] and are propagated to the simulation-based estimates of background yields and signal efficiencies. The combined effect of all photon uncertainties on the predicted signal efficiency and predicted number of events from single and double Higgs boson processes is about 2.5% in both the signal regions. Once incorporated into the fit and taking into account the effect on both the yields and the PNN shapes on signal and backgrounds, these translate into an uncertainty of 2%–4.5% in the signal sensitivity.

The category of jet-related uncertainties include uncertainties in the jet energy scale and jet energy resolution. These are derived using data-driven techniques [74] and compared with their counterpart in simulation. These uncertainties are propagated to the signal efficiency and background estimates. The combined effect of all jet-related uncertainties is largest in the 2 b-tagged signal region with up to 14% uncertainty in the signal efficiency for models with low m_S and decreasing to about 2% at high m_S. In the 1 b-tagged signal region that uncertainty remains smaller than 3%. The corresponding uncertainty in the predicted number of single and double Higgs boson processes is 5% (7%) in the 1 b-tagged (2 b-tagged) signal region. However the effect of these systematic uncertainties on the PNN shape remains small, of the order of 1% in the most signal-like PNN bin. Once incorporated into the fit and taking into account the effect on both the yields and the PNN shapes of signal and backgrounds, these translate into an uncertainty of about 1.5% in the signal sensitivity for $m_S > 110$ GeV. The impact grows at lower masses where it can reach up to 15%.

The category of pile-up related uncertainties comes from the reweighting of the MC simulation to the pile-up profile in data. This results in an uncertainty of at most 1% in the predicted number of events from Higgs boson processes. The effect on the signal efficiency is smaller than 1% in both the signal regions and for most of the parameter space, except in the 2 b-tagged signal region for low m_X where it can reach 1.8%. Finally the 0.83% uncertainty in the measured ATLAS Run 2 integrated luminosity is propagated to all processes normalised with their theoretical cross sections.

7.2 Theoretical systematic uncertainties

Theoretical systematic uncertainties affect the backgrounds normalised by their theoretical cross sections, but also the signal efficiency, and the non-resonant diphoton background. The latter is discussed in section 7.3.

For processes with significant contributions to the 1 b-tagged and 2 b-tagged signal regions and where the dominant heavy-flavour production is already taken into account at LO (ttH and ZH), several theoretical systematic uncertainties are considered. Scale uncertainties due to missing higher-order corrections in the production rates are estimated by varying the factorisation and renormalisation scales up and down from their nominal values by a factor two, taking the envelope of these variations. Parton shower uncertainties are evaluated by comparing against alternative samples where the parton shower is performed with Herwig 7.1.5 [90, 91]. The resulting bin-to-bin variations of the PNN output range from a few percent up to 10% in some bins, while the resulting impact on the exclusion limits is below 1%. Effects of the choice of PDF and α_S are estimated by varying them following the prescription in ref. [41]. These systematic uncertainties can lead to up to 5% bin-to-bin variations in the shape of the PNN discriminant output, but have a small impact on the limits.

For smaller Higgs boson backgrounds where the dominant heavy flavour production occurs at LO, the inclusive cross section uncertainties from ref. [56] are used along with scale, parton

JHEP11(2024)047

shower, PDF and α_S uncertainties derived as described above. The same procedure is followed for the $Z(\to q\bar{q})\gamma\gamma$ process. The final impact of these uncertainties on the results is small.

In single Higgs boson processes where b-quarks are not produced at LO (VBF H, WH, ggF H), a single 100% normalisation uncertainty is used. This is motivated by studies of heavy-flavour production in association with top-quark pairs [92, 93] and of W-boson production in association with b-jets [94]. These have a very small impact on the final sensitivity, except when searching for models with low m_S, where the 100% uncertainty in ggF H can lead to a 10% decrease in sensitivity to the signal.

The uncertainties in the Higgs boson decay branching ratios $BR(H \to \gamma\gamma)$ and $BR(H \to b\bar{b})$ propagate to the background yields, impacting the $\sigma(X \to SH \to b\bar{b}\gamma\gamma)$ limits by ∼3% and ∼1.5% respectively.

To better understand the overall impact of theoretical background systematic uncertainties, the limits on $\sigma(X \to SH \to b\bar{b}\gamma\gamma)$ are computed with and without the theoretical background systematic uncertainties described above. It is observed that the limits worsen by about 4% when including theoretical background systematic uncertainties. It can be noted that this is smaller than the effect of systematic uncertainties in the non-resonant diphoton background described in the next section and smaller than the effect of theoretical signal systematic uncertainties.

Theoretical systematic uncertainties are also considered for the $X \to S(\to b\bar{b})H(\to\gamma\gamma)$ signal, both in terms of the shape of the PNN output and the predicted event yields. They include scale, parton shower, PDF and α_S uncertainties calculated as described earlier. The impact of these systematic uncertainties on the signal efficiency and the shape of the PNN output are taken into account. These uncertainties lead to 2%–10% bin-to-bin variations of the PNN output shape, it is most pronounced for the parton shower uncertainty. The systematic uncertainties obtained by changing to an alternative PDF and α_S lead to up to 11% change in the predicted signal yield, particularly at high m_X ∼1000 GeV. The impact of theoretical signal uncertainties on the sensitivity to $\sigma(X \to SH \to b\bar{b}\gamma\gamma)$ can reach 10%. A systematic uncertainty associated with the interpolation of the PNN score in the region m_X >300 GeV and m_S >70 GeV is estimated by considering a shape systematic uncertainty in the PNN score, derived by varying the parameters of the Bukin probabilities within their errors. The impact on the exclusion limits at interpolated (m_X,m_S) points is at most 10%.

7.3 Systematic uncertainties in the non-resonant diphoton background

The normalisation of the non-resonant diphoton background is derived in a fit which includes the sideband control regions. The following theoretical uncertainties, introduced earlier, affect the PNN output shape and the overall estimated number of events in the signal and sideband regions: scale uncertainties, choice of PDF, α_s and parton shower. The uncertainties associated with the scales, PDFs and α_s are calculated using the same methods as described in section 7.2. The parton shower uncertainties are evaluated by using alternative samples generated with MadGraph [35] for the parton shower. An additional MC modelling uncertainty is considered by using an alternative $\gamma\gamma$+jets sample generated with MadGraph5_aMC@NLO. This sample models diphoton production with up to two jets at NLO. The corresponding uncertainty is found to be the most significant in the analysis; its impact in the 2 b-tagged signal region

JHEP11(2024)047

degrades the expected upper limits on the signal by up to 20%. This impact is larger for low values of m_X, while for m_X above 600 GeV the impact is always below 5%. For the 1 b-tagged signal region the modelling uncertainty has an impact of a few percent on the upper limits, except for two signal points at (500, 30) GeV and (230, 15) GeV where the effect is around 40% due to statistical fluctuations in the alternative MadGraph samples.

8 Results

8.1 Statistical model

The results of the analysis are obtained from a maximum-likelihood fit of the binned PNN output distribution, performed simultaneously over a signal region and its corresponding sideband region. The PNN binning is constructed starting from the rightmost signal-like bin. The size of this bin is chosen to maximise the signal-to-background ratio and widened until there is at least one background event. The same procedure is repeated with the next bin, and requiring that the number of background events is above a certain threshold, in order to avoid bins with large statistical errors. When the signal-to-background ratio in the bin drops below that of the full un-binned distribution, the iterative process is stopped and a single background-like bin is constructed for the remaining distribution at PNN outputs close to zero. The binning is optimised independently for each signal hypothesis. For the 1 b-jet selection a similar method is used.

The likelihood function is defined as:

$$\begin{aligned}\mathcal{L} = &\,\mathrm{Pois}\left(n_{\mathrm{SB}} \middle| \mu_{\gamma\gamma} N^{\gamma\gamma}_{\mathrm{SB}}(\boldsymbol{\theta}) + \sum_p N^p_{\mathrm{SB}}(\boldsymbol{\theta})\right) \\ &\cdot \prod_i \mathrm{Pois}\left(n_{\mathrm{SR},i} \middle| \mu_{\gamma\gamma} N^{\gamma\gamma}_{\mathrm{SR}}(\boldsymbol{\theta}) f^{\gamma\gamma}_i(\boldsymbol{\theta}) + \sum_p N^p_{\mathrm{SR}}(\boldsymbol{\theta}) f^p_i(\boldsymbol{\theta})\right) \cdot G(\boldsymbol{\theta})\end{aligned} \tag{8.1}$$

where the index p runs over physics processes other than $\gamma\gamma$+jets, the index i runs over the bins of the PNN output, $n_{\mathrm{SR},i}$ and n_{SB} are the observed number of events in the signal region PNN bin i and in the corresponding sideband region, $N^p_{\mathrm{SR}}(\boldsymbol{\theta})$ is the expected number of events from process p in the signal region, and $N_{\mathrm{SB}}(\boldsymbol{\theta})$ is the total expected number of events in the corresponding sideband region. The superscript $\gamma\gamma$ is used for parameters that specifically apply to the $\gamma\gamma$+jets background. The factor $\mu_{\gamma\gamma}$ is the free parameter that fits the $\gamma\gamma$+jets normalisation to the data. The function f^p_i gives the shape or probability density function (pdf) of the PNN output discriminant for each background or signal process; therefore $N^p_{\mathrm{SR}} f^p_i$ is the expected number of events of process p in the PNN bin i. Finally $\boldsymbol{\theta}$ is a vector of nuisance parameters, and $G(\boldsymbol{\theta})$ are constrained pdfs for the nuisance parameters. Correlation of the nuisance parameters across different signal and background components, as well as categories, is taken into account.

The nominal yields of the single and double Higgs boson background processes are initially set to values from simulation. The likelihood function includes all the nuisance parameters that describe the systematic uncertainties. The signal cross section is a free parameter in the fit. The measurement of the parameter of interest is carried out using a statistical test based on the profile likelihood ratio [95]. In the absence of signal, upper

JHEP11(2024)047

limits on $\sigma(X \to SH \to b\bar{b}\gamma\gamma)$ at the 95% CL are set. The limits are calculated using the asymptotic formula with a profile-likelihood-ratio-based test statistic [95], and are based on the CL_S method [96]. The binning in PNN score was chosen to ensure that the asymptotic approximation would be valid.

8.2 Control region validation

The ability of the background model to reproduce the data is studied in the sideband regions where a background-only fit is performed to the data. Distributions are then compared between the post-fit model and the data as shown in figure 2. A good agreement between the data and the model shows the ability of the model to reproduce the PNN discriminant output in both the 2 b-tagged and 1 b-tagged regions. For each value of $\bar{\theta} = (m_S, m_X)$ the PNN($\bar{\theta}$) is effectively a different observable, for this reason the post-fit data-to-prediction comparison in the sideband is performed for all analysed signal mass points, and good agreement is observed.

8.3 Result and interpretation

The results of the background-only fit in the signal regions and sidebands to the data is shown in table 2. The signal region and sideband yields are independent of the parameterised neural network, while the column "Signal-like bin" illustrates the signal and background yields in the most signal-like bin of the PNN for two choices of $\bar{\theta}$, namely (250, 100) GeV and (1000, 70) GeV. Figure 3 illustrates the post-fit distribution of the PNN in the 2 b-tagged and 1 b-tagged regions at two different $\bar{\theta}$. PNN($\bar{\theta}$) is sensitive not only to a signal at the same masses defined by $\bar{\theta}$, but also to signals with nearby masses $\bar{\theta}'$. To check for discovery of a wide range of signal masses, the background-only hypothesis is tested against the data for a highly granular grid of PNN parameters $\bar{\theta}$. The step size between two consecutive parameters $\bar{\theta}$ is selected by studying the sensitivity of PNN($\bar{\theta}$) to a signal with different masses $\bar{\theta}'$. If there was an excess in data due to a signal with masses $\bar{\theta}'$ observed with the discriminant PNN($\bar{\theta}$), the significance of this excess would degrade with increasing distance between $\bar{\theta}'$ and $\bar{\theta}$. A step size in the $\bar{\theta}$ grid is chosen such that the degradation of the significance does not exceed 10% between two consecutive grid points. In practice the step size goes from 5 GeV in the densest regions to 25 GeV for $m_X \geq 250$ GeV, and to 50 GeV for $m_X \geq 600$ GeV and $m_S \geq 200$ GeV.

For most mass points good agreement is observed between data and the SM background-only expectation; however some deviation is observed for a few points. The largest excess of the observation over the SM background-only hypothesis occurs for $(m_X, m_S) = (575, 200)$ GeV with a local significance of 3.5σ. The 'look-elsewhere effect' is taken into account using the asymptotic method described in ref. [97]. An asymptotic formula for the Euler characteristic as a function of the maximum of the test statistic across each signal point is derived using toy MC experiments. The resulting global significance is calculated to be 2.0σ. At this mass point the signal PNN output shape was initially derived from interpolation. The analysis was repeated using a simulated sample; the observed significance remained however unchanged, confirming the validity of the interpolation method.

A parameter point of particular interest is $(m_X, m_S) = (650, 90)$ GeV where the CMS Collaboration reports a deviation between observation and background-only expectation, corresponding to a local (global) significance of 3.8 (2.8) standard deviations [17]. Injecting

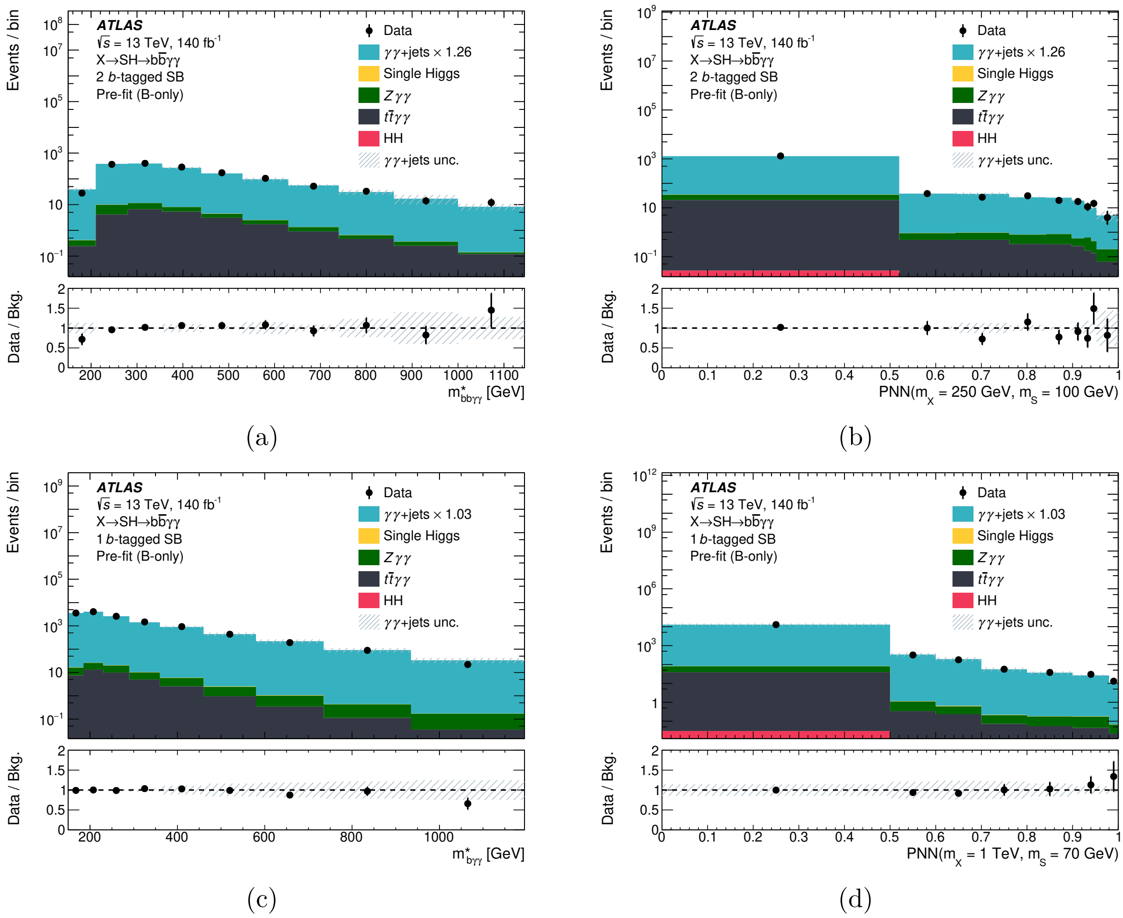

Figure 2. Distributions of (a) $m^*_{bb\gamma\gamma}$, (c) $m^*_{b\gamma\gamma}$ and (b,d) PNN for two choices of $\bar{\theta} = (m_S, m_X)$ in data and in the predicted model, in the sidebands of the 2 b-tagged region (top) and 1 b-tagged region (bottom). The $\gamma\gamma$ + jets background is rescaled to its post-fit normalisation in a background-only fit. The variables $m^*_{bb\gamma\gamma}$ and $m^*_{b\gamma\gamma}$ are defined as $m^*_{bb\gamma\gamma} = m_{bb\gamma\gamma} - (m_{\gamma\gamma} - 125\text{ GeV})$ and $m^*_{b\gamma\gamma} = m_{b\gamma\gamma} - (m_{\gamma\gamma} - 125\text{ GeV})$. The $\gamma\gamma$ + jets category represents the sum of $\gamma\gamma$ + jets, γ + jets and dijet backgrounds. The error band corresponds to the dominant uncertainty, which arises from the non-resonant $\gamma\gamma$ + jets background.

a MC signal with a production cross section of 0.35 fb (the best fit reported by the CMS experiment) in the analysis performed in this paper yields a local excess in observation to SM expectation of 2.7 standard deviations, demonstrating the sensitivity of this analysis to a signal consistent with the excess observed by CMS. The results of the analysis of ATLAS data for this specific parameter point instead shows good agreement between observation and SM background expectation (the p-value of the background-only hypothesis is larger than 0.5). The 95% CL upper limit on $\sigma(X \to SH \to b\bar{b}\gamma\gamma)$ for this specific mass point is 0.2 fb.

The statistical analysis sets 95% CL upper limits on $\sigma(X \to SH \to b\bar{b}\gamma\gamma)$ for all values of $\bar{\theta} = (m_X, m_S)$ by performing a signal-plus-background fit to the PNN output distribution in data. For each mass point the signal region which gives the best expected upper limit is selected. The resulting expected and observed upper limits are presented in figure 4, and range from observed (expected) limits of 39 (25) fb at m_X = 170 GeV and m_S = 30 GeV,

JHEP11(2024)047

Background	2 b-tagged region Sideband	Signal region	Signal-like bin	1 b-tagged region Sideband	Signal region	Signal-like bin
Non-res. $\gamma\gamma$	1480 ± 37	372 ± 16	1.64 ± 0.37	13450 ± 110	3392 ± 53	2.45 ± 0.43
Single Higgs	0.46 ± 0.11	19.9 ± 5.3	0.04 ± 0.01	2.3 ± 1.1	92 ± 44	0.21 ± 0.10
ggF+$b\bar{b}H$	0.14 ± 0.11	6.5 ± 5.2	0.01 ± 0.01	1.5 ± 1.1	56 ± 43	0.11 ± 0.09
$t\bar{t}H$	0.21 ± 0.01	7.91 ± 0.77	0.01 ± 0.01	0.31 ± 0.01	11.4 ± 1.1	0.03 ± 0.01
ZH	0.08 ± 0.01	3.56 ± 0.30	0.02 ± 0.01	0.17 ± 0.01	7.35 ± 0.60	0.02 ± 0.01
Other	0.03 ± 0.01	1.94 ± 0.70	< 0.005	0.40 ± 0.23	17 ± 10	0.05 ± 0.03
Double Higgs	0.03 ± 0.01	1.65 ± 0.25	< 0.005	0.03 ± 0.01	1.79 ± 0.27	0.01 ± 0.01
Total	1480 ± 37	394 ± 16	1.67 ± 0.37	13450 ± 110	3486 ± 48	2.67 ± 0.45
Signal (m_X, m_S)						
(250, 100) GeV	0.38 ± 0.04	8.3 ± 1.2	1.43 ± 0.21			
(1000, 70) GeV				0.97 ± 0.10	33.3 ± 5.8	23.9 ± 4.2
Data	1479	395	0	13450	3491	4

Table 2. Number of events for the different process categories obtained from a background-only fit to data in the signal regions and sidebands. Observed and fitted event yields in the two signal regions and sidebands, independent of phase space parameters $\bar{\theta}$, are given in the columns "Signal region" and "Sideband". The yields in the most signal-like bin of the PNN distribution depend on the selected phase space parameters $\bar{\theta}$, here shown under the column "Signal-like bin" for $\bar{\theta} = (m_X, m_S)$ = (250, 100) GeV and (1000, 70) GeV. The expected number of events from the two corresponding benchmark signals with a 1 fb cross section is also given. The uncertainties are symmetrised around the central value. The uncertainty in the total background is calculated taking correlations between the individual contributions into account. For the single Higgs boson processes, "Other" includes the following production modes: VBF, WH, tHq, and tHW.

to 0.09 (0.14) fb at $m_X = 1000$ GeV and m_S between 250 and 300 GeV. The upper limits improve at higher masses, consistent with the fact that signals with higher m_X become easier to differentiate from SM processes. In contrast, they worsen in the boosted signal regime at lower m_S, where the 1 b-tagged region is employed, and consistent with the lower signal-to-background ratio shown in table 2 for the 1 b-tagged region. At low m_X the sensitivity suffers from an increasing fraction of b-jets falling below the jet p_{T} reconstruction threshold.

9 Conclusion

A search for a signal from a hypothetical scalar X is performed, considering the case where it decays into another hypothetical scalar S and a Higgs boson, which subsequently decay into pairs of b-quarks and photons, respectively. Two signal regions targeting resolved or boosted $S \to b\bar{b}$ decays are analysed using parameterised neural networks, which provide continuous sensitivity in the probed (m_X, m_S) plane. In the region $m_X > 300$ GeV and $m_S > 70$ GeV the validity of the limits for intermediate mass points is ensured by interpolating the signal shapes to a much finer signal grid, and the finer grid spacing is guided by the sensitivity range of the PNN to values of (m_X, m_S) where it was not trained. At lower masses the validity of the limits for intermediate mass points is ensured by using a very fine grid of simulated signal samples.

JHEP11(2024)047

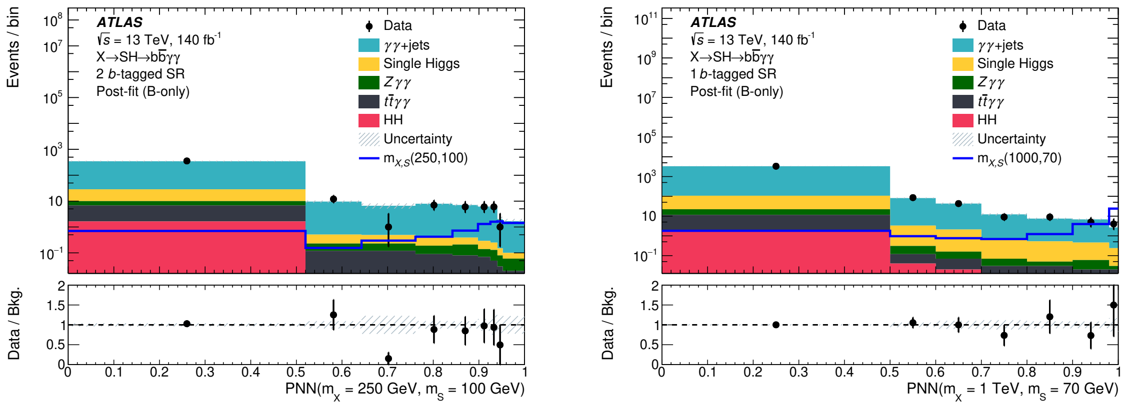

(a) (b)

Figure 3. Post-fit distributions of the PNN discriminant output in the (a) 2 b-tagged signal region for $m_X = 250$ GeV and $m_S = 100$ GeV and (b) 1 b-tagged signal region for $m_X = 1000$ GeV and $m_S = 70$ GeV, after a background-only fit to data. The signals corresponding to the two PNN parameterisations, normalised to a 1 fb cross section, are illustrated for comparison. The $\gamma\gamma$+ jets category represents the sum of $\gamma\gamma$+ jets, γ + jets and dijet backgrounds. The error band corresponds to the total systematic uncertainty after fit.

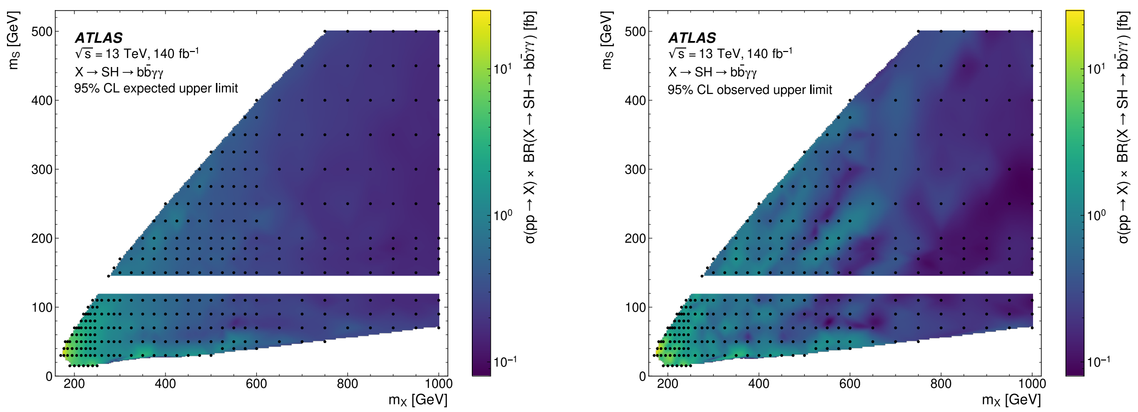

(a) (b)

Figure 4. (a) Expected and (b) observed 95% CL upper limits on the signal cross section times branching fraction for the $X \to SH$ signal, in the (m_X, m_S) plane. The points show where the limits were evaluated. The band at $m_S = 125$ GeV is not shown as those points are equivalent to those already probed in ref. [19].

No significant excess with respect to the Standard Model background is found. Therefore, 95% CL upper limits are set on $\sigma(X \to SH \to b\bar{b}\gamma\gamma)$ in the ranges $170 \leq m_X \leq 1000$ GeV and $15 \leq m_S \leq 500$ GeV, expanding earlier LHC results to lower masses and providing higher sensitivity. The largest deviation from the background-only expectation occurs for $(m_X, m_S) = (575, 200)$ GeV with a local (global) significance of 3.5 (2.0) standard deviations. For the mass point $(m_X, m_S) = (650, 90)$ GeV, where CMS reported an excess with a local (global) significance of 3.8 (2.8) standard deviations, this analysis shows good agreement with the background-only hypothesis and sets a 95% CL upper limit on the signal cross section of 0.2 fb.

Acknowledgments

We thank CERN for the very successful operation of the LHC and its injectors, as well as the support staff at CERN and at our institutions worldwide without whom ATLAS could not be operated efficiently.

The crucial computing support from all WLCG partners is acknowledged gratefully, in particular from CERN, the ATLAS Tier-1 facilities at TRIUMF/SFU (Canada), NDGF (Denmark, Norway, Sweden), CC-IN2P3 (France), KIT/GridKA (Germany), INFN-CNAF (Italy), NL-T1 (Netherlands), PIC (Spain), RAL (UK) and BNL (USA), the Tier-2 facilities worldwide and large non-WLCG resource providers. Major contributors of computing resources are listed in ref. [98].

We gratefully acknowledge the support of ANPCyT, Argentina; YerPhI, Armenia; ARC, Australia; BMWFW and FWF, Austria; ANAS, Azerbaijan; CNPq and FAPESP, Brazil; NSERC, NRC and CFI, Canada; CERN; ANID, Chile; CAS, MOST and NSFC, China; Minciencias, Colombia; MEYS CR, Czech Republic; DNRF and DNSRC, Denmark; IN2P3-CNRS and CEA-DRF/IRFU, France; SRNSFG, Georgia; BMBF, HGF and MPG, Germany; GSRI, Greece; RGC and Hong Kong SAR, China; ISF and Benoziyo Center, Israel; INFN, Italy; MEXT and JSPS, Japan; CNRST, Morocco; NWO, Netherlands; RCN, Norway; MEiN, Poland; FCT, Portugal; MNE/IFA, Romania; MESTD, Serbia; MSSR, Slovakia; ARIS and MVZI, Slovenia; DSI/NRF, South Africa; MICINN, Spain; SRC and Wallenberg Foundation, Sweden; SERI, SNSF and Cantons of Bern and Geneva, Switzerland; NSTC, Taipei; TENMAK, Türkiye; STFC/UKRI, United Kingdom; DOE and NSF, United States of America.

Individual groups and members have received support from BCKDF, CANARIE, CRC and DRAC, Canada; CERN-CZ, PRIMUS 21/SCI/017 and UNCE SCI/013, Czech Republic; COST, ERC, ERDF, Horizon 2020, ICSC-NextGenerationEU and Marie Skłodowska-Curie Actions, European Union; Investissements d'Avenir Labex, Investissements d'Avenir Idex and ANR, France; DFG and AvH Foundation, Germany; Herakleitos, Thales and Aristeia programmes co-financed by EU-ESF and the Greek NSRF, Greece; BSF-NSF and MINERVA, Israel; Norwegian Financial Mechanism 2014-2021, Norway; NCN and NAWA, Poland; La Caixa Banking Foundation, CERCA Programme Generalitat de Catalunya and PROMETEO and GenT Programmes Generalitat Valenciana, Spain; Göran Gustafssons Stiftelse, Sweden; The Royal Society and Leverhulme Trust, United Kingdom.

In addition, individual members wish to acknowledge support from CERN: European Organization for Nuclear Research (CERN PJAS); Chile: Agencia Nacional de Investigación y Desarrollo (FONDECYT 1190886, FONDECYT 1210400, FONDECYT 1230812, FONDECYT 1230987); China: National Natural Science Foundation of China (NSFC - 12175119, NSFC 12275265, NSFC-12075060); Czech Republic: PRIMUS Research Programme (PRIMUS/21/SCI/017); EU: H2020 European Research Council (ERC - 101002463); European Union: European Research Council (ERC - 948254, ERC 101089007), Horizon 2020 Framework Programme (MUCCA - CHIST-ERA-19-XAI-00), European Union, Future Artificial Intelligence Research (FAIR-NextGenerationEU PE00000013), Italian Center for High Performance Computing, Big Data and Quantum Computing (ICSC, NextGenerationEU); France: Agence Nationale de la Recherche (ANR-20-CE31-0013, ANR-21-CE31-0013, ANR-21-CE31-0022, ANR-22-EDIR-0002), Investissements d'Avenir Labex (ANR-11-LABX-0012); Germany: Baden-Württemberg Stiftung (BW Stiftung-Postdoc Eliteprogramme), Deutsche Forschungsgemeinschaft (DFG - 469666862, DFG - CR 312/5-2); Italy: Istituto Nazionale di Fisica Nucleare (ICSC, NextGenerationEU), Ministero dell'Università e della Ricerca (PRIN - 20223N7F8K - PNRR M4.C2.1.1); Japan: Japan Society for the Promotion of Science (JSPS KAKENHI JP21H05085, JSPS KAKENHI JP22H01227, JSPS KAKENHI JP22H04944, JSPS KAKENHI JP22KK0227); Netherlands: Netherlands Organisation for Scientific Research (NWO Veni 2020 - VI.Veni.202.179); Norway: Research Council of Norway (RCN-314472); Poland: Polish National Agency for Academic Exchange (PPN/PPO/2020/1/00002/U/00001), Polish National Science Centre (NCN 2021/42/E/ST2/00350, NCN OPUS nr 2022/47/B/ST2/03059, NCN UMO-2019/34/E/ST2/00393, UMO-2020/37/B/ST2/01043, UMO-2021/40/C/ST2/00187, UMO-2022/47/O/ST2/00148); Slovenia: Slovenian Research Agency (ARIS grant J1-3010); Spain: BBVA Foundation (LEO22-1-603), Generalitat Valenciana (Artemisa, FEDER, IDIFEDER/2018/048), La Caixa Banking Foundation (LCF/BQ/PI20/11760025), Ministry of Science and Innovation (MCIN & NextGenEU PCI2022-135018-2, MICIN & FEDER PID2021-125273NB, RYC2019-028510-I, RYC2020-030254-I, RYC2021-031273-I, RYC2022-038164-I), PROMETEO and GenT Programmes Generalitat Valenciana (CIDEGENT/2019/023, CIDEGENT/2019/027); Sweden: Swedish Research Council (VR 2018-00482, VR 2022-03845, VR 2022-04683, VR grant 2021-03651), Knut and Alice Wallenberg Foundation (KAW 2017.0100, KAW 2018.0157, KAW 2018.0458, KAW 2019.0447, KAW 2022.0358); Switzerland: Swiss National Science Foundation (SNSF - PCEFP2_194658); United Kingdom: Leverhulme Trust (Leverhulme Trust RPG-2020-004); United States of America: U.S. Department of Energy (ECA DE-AC02-76SF00515), Neubauer Family Foundation.

References

[1] ATLAS collaboration, *Observation of a new particle in the search for the Standard Model Higgs boson with the ATLAS detector at the LHC*, *Phys. Lett. B* **716** (2012) 1 [arXiv:1207.7214] [INSPIRE].

[2] CMS collaboration, *Observation of a New Boson at a Mass of 125 GeV with the CMS Experiment at the LHC*, *Phys. Lett. B* **716** (2012) 30 [arXiv:1207.7235] [INSPIRE].

[3] CMS collaboration, *A portrait of the Higgs boson by the CMS experiment ten years after the discovery*, *Nature* **607** (2022) 60 [arXiv:2207.00043] [INSPIRE].

[4] ATLAS collaboration, *A detailed map of Higgs boson interactions by the ATLAS experiment ten years after the discovery*, *Nature* **607** (2022) 52 [*Erratum ibid.* **612** (2022) E24] [arXiv:2207.00092] [INSPIRE].

[5] A. Ferrari and N. Rompotis, *Exploration of Extended Higgs Sectors with Run-2 Proton–Proton Collision Data at the LHC*, *Symmetry* **13** (2021) 2144 [*Erratum ibid.* **14** (2022) 1546] [INSPIRE].

[6] V. Barger et al., *Complex Singlet Extension of the Standard Model*, *Phys. Rev. D* **79** (2009) 015018 [arXiv:0811.0393] [INSPIRE].

[7] T. Robens, T. Stefaniak and J. Wittbrodt, *Two-real-scalar-singlet extension of the SM: LHC phenomenology and benchmark scenarios*, *Eur. Phys. J. C* **80** (2020) 151 [arXiv:1908.08554] [INSPIRE].

[8] I.F. Ginzburg, M. Krawczyk and P. Osland, *Two Higgs doublet models with CP violation*, in the proceedings of the *International Workshop on Linear Colliders (LCWS 2002)*, Jeju Island, South Korea, August 26–30 (2002) [hep-ph/0211371] [INSPIRE].

[9] X.-G. He et al., *Constraints on Scalar Dark Matter from Direct Experimental Searches*, *Phys. Rev. D* **79** (2009) 023521 [arXiv:0811.0658] [INSPIRE].

[10] M. Muhlleitner, M.O.P. Sampaio, R. Santos and J. Wittbrodt, *The N2HDM under Theoretical and Experimental Scrutiny*, *JHEP* **03** (2017) 094 [arXiv:1612.01309] [INSPIRE].

[11] U. Ellwanger, C. Hugonie and A.M. Teixeira, *The Next-to-Minimal Supersymmetric Standard Model*, *Phys. Rept.* **496** (2010) 1 [arXiv:0910.1785] [INSPIRE].

[12] M. Maniatis, *The Next-to-Minimal Supersymmetric extension of the Standard Model reviewed*, *Int. J. Mod. Phys. A* **25** (2010) 3505 [arXiv:0906.0777] [INSPIRE].

[13] P. Basler, S. Dawson, C. Englert and M. Mühlleitner, *Showcasing HH production: Benchmarks for the LHC and HL-LHC*, *Phys. Rev. D* **99** (2019) 055048 [arXiv:1812.03542] [INSPIRE].

[14] S. Baum and N.R. Shah, *Benchmark Suggestions for Resonant Double Higgs Production at the LHC for Extended Higgs Sectors*, arXiv:1904.10810 [INSPIRE].

[15] CMS collaboration, *Search for a massive scalar resonance decaying to a light scalar and a Higgs boson in the four b quarks final state with boosted topology*, *Phys. Lett. B* **842** (2023) 137392 [arXiv:2204.12413] [INSPIRE].

[16] CMS collaboration, *Search for a heavy Higgs boson decaying into two lighter Higgs bosons in the $\tau\tau bb$ final state at 13 TeV*, *JHEP* **11** (2021) 057 [arXiv:2106.10361] [INSPIRE].

[17] CMS collaboration, *Search for a new resonance decaying into two spin-0 bosons in a final state with two photons and two bottom quarks in proton-proton collisions at $\sqrt{s} = 13$ TeV*, *JHEP* **05** (2024) 316 [arXiv:2310.01643] [INSPIRE].

[18] ATLAS collaboration, *Search for a new heavy scalar particle decaying into a Higgs boson and a new scalar singlet in final states with one or two light leptons and a pair of τ-leptons with the ATLAS detector*, *JHEP* **10** (2023) 009 [arXiv:2307.11120] [INSPIRE].

[19] ATLAS collaboration, *Search for Higgs boson pair production in the two bottom quarks plus two photons final state in pp collisions at $\sqrt{s} = 13$ TeV with the ATLAS detector*, *Phys. Rev. D* **106** (2022) 052001 [arXiv:2112.11876] [INSPIRE].

[20] ATLAS collaboration, *The ATLAS Experiment at the CERN Large Hadron Collider*, 2008 *JINST* **3** S08003 [INSPIRE].

[21] ATLAS collaboration, *ATLAS Insertable B-Layer Technical Design Report*, CERN-LHCC-2010-013, (2010) [Addendum: CERN-LHCC-2012-009, (2012)].

[22] ATLAS IBL collaboration, *Production and Integration of the ATLAS Insertable B-Layer*, 2018 *JINST* **13** T05008 [arXiv:1803.00844] [INSPIRE].

[23] G. Avoni et al., *The new LUCID-2 detector for luminosity measurement and monitoring in ATLAS*, 2018 *JINST* **13** P07017 [INSPIRE].

[24] ATLAS collaboration, *Performance of the ATLAS Trigger System in 2015*, *Eur. Phys. J. C* **77** (2017) 317 [arXiv:1611.09661] [INSPIRE].

[25] ATLAS collaboration, *The ATLAS Collaboration Software and Firmware*, ATL-SOFT-PUB-2021-001, CERN, Geneva (2021).

[26] ATLAS collaboration, *ATLAS data quality operations and performance for 2015–2018 data-taking*, 2020 *JINST* **15** P04003 [arXiv:1911.04632] [INSPIRE].

[27] ATLAS collaboration, *Luminosity determination in pp collisions at $\sqrt{s} = 13$ TeV using the ATLAS detector at the LHC*, *Eur. Phys. J. C* **83** (2023) 982 [arXiv:2212.09379] [INSPIRE].

[28] ATLAS collaboration, *Performance of electron and photon triggers in ATLAS during LHC Run 2*, *Eur. Phys. J. C* **80** (2020) 47 [arXiv:1909.00761] [INSPIRE].

[29] ATLAS collaboration, *Electron and photon performance measurements with the ATLAS detector using the 2015–2017 LHC proton-proton collision data*, 2019 *JINST* **14** P12006 [arXiv:1908.00005] [INSPIRE].

[30] T. Sjöstrand et al., *An introduction to PYTHIA 8.2*, *Comput. Phys. Commun.* **191** (2015) 159 [arXiv:1410.3012] [INSPIRE].

[31] R.D. Ball et al., *Parton distributions with LHC data*, *Nucl. Phys. B* **867** (2013) 244 [arXiv:1207.1303] [INSPIRE].

[32] ATLAS collaboration, *ATLAS Pythia 8 tunes to 7 TeV data*, ATL-PHYS-PUB-2014-021, CERN, Geneva (2014).

[33] SHERPA collaboration, *Event Generation with Sherpa 2.2*, *SciPost Phys.* **7** (2019) 034 [arXiv:1905.09127] [INSPIRE].

[34] NNPDF collaboration, *Parton distributions for the LHC Run II*, *JHEP* **04** (2015) 040 [arXiv:1410.8849] [INSPIRE].

[35] J. Alwall et al., *The automated computation of tree-level and next-to-leading order differential cross sections, and their matching to parton shower simulations*, *JHEP* **07** (2014) 079 [arXiv:1405.0301] [INSPIRE].

[36] K. Hamilton, P. Nason and G. Zanderighi, *MINLO: Multi-Scale Improved NLO*, *JHEP* **10** (2012) 155 [arXiv:1206.3572] [INSPIRE].

[37] J.M. Campbell et al., *NLO Higgs Boson Production Plus One and Two Jets Using the POWHEG BOX, MadGraph4 and MCFM*, *JHEP* **07** (2012) 092 [arXiv:1202.5475] [INSPIRE].

[38] K. Hamilton, P. Nason, C. Oleari and G. Zanderighi, *Merging H/W/Z + 0 and 1 jet at NLO with no merging scale: a path to parton shower + NNLO matching*, *JHEP* **05** (2013) 082 [arXiv:1212.4504] [INSPIRE].

[39] G. Bozzi, S. Catani, D. de Florian and M. Grazzini, *Transverse-momentum resummation and the spectrum of the Higgs boson at the LHC*, *Nucl. Phys. B* **737** (2006) 73 [hep-ph/0508068] [INSPIRE].

[40] D. de Florian, G. Ferrera, M. Grazzini and D. Tommasini, *Transverse-momentum resummation: Higgs boson production at the Tevatron and the LHC*, *JHEP* **11** (2011) 064 [arXiv:1109.2109] [INSPIRE].

[41] J. Butterworth et al., *PDF4LHC recommendations for LHC Run II*, *J. Phys. G* **43** (2016) 023001 [arXiv:1510.03865] [INSPIRE].

[42] ATLAS collaboration, *Measurement of the Z/γ^* boson transverse momentum distribution in pp collisions at $\sqrt{s} = 7$ TeV with the ATLAS detector*, *JHEP* **09** (2014) 145 [arXiv:1406.3660] [INSPIRE].

[43] P. Nason, *A new method for combining NLO QCD with shower Monte Carlo algorithms*, *JHEP* **11** (2004) 040 [hep-ph/0409146] [INSPIRE].

[44] S. Frixione, P. Nason and C. Oleari, *Matching NLO QCD computations with Parton Shower simulations: the POWHEG method*, *JHEP* **11** (2007) 070 [arXiv:0709.2092] [INSPIRE].

[45] S. Alioli, P. Nason, C. Oleari and E. Re, *A general framework for implementing NLO calculations in shower Monte Carlo programs: the POWHEG BOX*, *JHEP* **06** (2010) 043 [arXiv:1002.2581] [INSPIRE].

[46] P. Nason and C. Oleari, *NLO Higgs boson production via vector-boson fusion matched with shower in POWHEG*, *JHEP* **02** (2010) 037 [arXiv:0911.5299] [INSPIRE].

[47] K. Mimasu, V. Sanz and C. Williams, *Higher Order QCD predictions for Associated Higgs production with anomalous couplings to gauge bosons*, *JHEP* **08** (2016) 039 [arXiv:1512.02572] [INSPIRE].

[48] G. Luisoni, P. Nason, C. Oleari and F. Tramontano, *$HW^{\pm}/HZ$ + 0 and 1 jet at NLO with the POWHEG BOX interfaced to GoSam and their merging within MiNLO*, *JHEP* **10** (2013) 083 [arXiv:1306.2542] [INSPIRE].

[49] H.B. Hartanto, B. Jager, L. Reina and D. Wackeroth, *Higgs boson production in association with top quarks in the POWHEG BOX*, *Phys. Rev. D* **91** (2015) 094003 [arXiv:1501.04498] [INSPIRE].

[50] G. Heinrich et al., *NLO predictions for Higgs boson pair production with full top quark mass dependence matched to parton showers*, *JHEP* **08** (2017) 088 [arXiv:1703.09252] [INSPIRE].

[51] G. Heinrich et al., *Probing the trilinear Higgs boson coupling in di-Higgs production at NLO QCD including parton shower effects*, *JHEP* **06** (2019) 066 [arXiv:1903.08137] [INSPIRE].

[52] T. Gleisberg and S. Hoeche, *Comix, a new matrix element generator*, *JHEP* **12** (2008) 039 [arXiv:0808.3674] [INSPIRE].

[53] F. Buccioni et al., *OpenLoops 2*, *Eur. Phys. J. C* **79** (2019) 866 [arXiv:1907.13071] [INSPIRE].

[54] F. Cascioli, P. Maierhofer and S. Pozzorini, *Scattering Amplitudes with Open Loops*, *Phys. Rev. Lett.* **108** (2012) 111601 [arXiv:1111.5206] [INSPIRE].

[55] A. Denner, S. Dittmaier and L. Hofer, *Collier: a fortran-based Complex One-Loop LIbrary in Extended Regularizations*, *Comput. Phys. Commun.* **212** (2017) 220 [arXiv:1604.06792] [INSPIRE].

[56] LHC Higgs Cross Section Working Group collaboration, *Handbook of LHC Higgs Cross Sections: 4. Deciphering the Nature of the Higgs Sector*, arXiv:1610.07922 [DOI:10.23731/CYRM-2017-002] [INSPIRE].

[57] J. Alison et al., *Higgs boson potential at colliders: Status and perspectives*, *Rev. Phys.* **5** (2020) 100045 [arXiv:1910.00012] [INSPIRE].

[58] D.Y. Shao, C.S. Li, H.T. Li and J. Wang, *Threshold resummation effects in Higgs boson pair production at the LHC*, *JHEP* **07** (2013) 169 [arXiv:1301.1245] [INSPIRE].

[59] D. de Florian and J. Mazzitelli, *Higgs pair production at next-to-next-to-leading logarithmic accuracy at the LHC*, *JHEP* **09** (2015) 053 [arXiv:1505.07122] [INSPIRE].

[60] J. Baglio et al., *$gg \to HH$: Combined uncertainties*, *Phys. Rev. D* **103** (2021) 056002 [arXiv:2008.11626] [INSPIRE].

[61] A. Djouadi, J. Kalinowski and M. Spira, *HDECAY: A Program for Higgs boson decays in the standard model and its supersymmetric extension*, *Comput. Phys. Commun.* **108** (1998) 56 [hep-ph/9704448] [INSPIRE].

[62] D.J. Lange, *The EvtGen particle decay simulation package*, *Nucl. Instrum. Meth. A* **462** (2001) 152 [INSPIRE].

[63] ATLAS collaboration, *The ATLAS Simulation Infrastructure*, *Eur. Phys. J. C* **70** (2010) 823 [arXiv:1005.4568] [INSPIRE].

[64] GEANT4 collaboration, *GEANT4–a simulation toolkit*, *Nucl. Instrum. Meth. A* **506** (2003) 250 [INSPIRE].

[65] ATLAS collaboration, *The simulation principle and performance of the ATLAS fast calorimeter simulation FastCaloSim*, ATL-PHYS-PUB-2010-013, CERN, Geneva (2010).

[66] T. Sjostrand, S. Mrenna and P.Z. Skands, *A Brief Introduction to PYTHIA 8.1*, *Comput. Phys. Commun.* **178** (2008) 852 [arXiv:0710.3820] [INSPIRE].

[67] ATLAS collaboration, *The Pythia 8 A3 tune description of ATLAS minimum bias and inelastic measurements incorporating the Donnachie-Landshoff diffractive model*, ATL-PHYS-PUB-2016-017, CERN, Geneva (2016).

[68] ATLAS collaboration, *Measurement of Higgs boson production in the diphoton decay channel in pp collisions at center-of-mass energies of 7 and 8 TeV with the ATLAS detector*, *Phys. Rev. D* **90** (2014) 112015 [arXiv:1408.7084] [INSPIRE].

[69] ATLAS collaboration, *Muon reconstruction performance of the ATLAS detector in proton–proton collision data at $\sqrt{s} = 13$ TeV*, *Eur. Phys. J. C* **76** (2016) 292 [arXiv:1603.05598] [INSPIRE].

[70] ATLAS collaboration, *Muon reconstruction and identification efficiency in ATLAS using the full Run 2 pp collision data set at $\sqrt{s} = 13$ TeV*, *Eur. Phys. J. C* **81** (2021) 578 [arXiv:2012.00578] [INSPIRE].

[71] ATLAS collaboration, *Jet reconstruction and performance using particle flow with the ATLAS Detector*, *Eur. Phys. J. C* **77** (2017) 466 [arXiv:1703.10485] [INSPIRE].

[72] M. Cacciari, G.P. Salam and G. Soyez, *The anti-k_t jet clustering algorithm*, *JHEP* **04** (2008) 063 [arXiv:0802.1189] [INSPIRE].

[73] M. Cacciari, G.P. Salam and G. Soyez, *FastJet User Manual*, *Eur. Phys. J. C* **72** (2012) 1896 [arXiv:1111.6097] [INSPIRE].

[74] ATLAS collaboration, *Jet energy scale and resolution measured in proton–proton collisions at $\sqrt{s} = 13$ TeV with the ATLAS detector*, *Eur. Phys. J. C* **81** (2021) 689 [arXiv:2007.02645] [INSPIRE].

[75] ATLAS collaboration, *Performance of pile-up mitigation techniques for jets in pp collisions at $\sqrt{s} = 8$ TeV using the ATLAS detector*, *Eur. Phys. J. C* **76** (2016) 581 [arXiv:1510.03823] [INSPIRE].

[76] ATLAS collaboration, *ATLAS flavour-tagging algorithms for the LHC Run 2 pp collision dataset*, *Eur. Phys. J. C* **83** (2023) 681 [arXiv:2211.16345] [INSPIRE].

[77] ATLAS collaboration, *Identification of Jets Containing b-Hadrons with Recurrent Neural Networks at the ATLAS Experiment*, ATL-PHYS-PUB-2017-003, CERN, Geneva (2017).

[78] ATLAS collaboration, *ATLAS b-jet identification performance and efficiency measurement with $t\bar{t}$ events in pp collisions at $\sqrt{s} = 13$ TeV*, *Eur. Phys. J. C* **79** (2019) 970 [arXiv:1907.05120] [INSPIRE].

[79] ATLAS collaboration, *Measurement of the c-jet mistagging efficiency in $t\bar{t}$ events using pp collision data at $\sqrt{s} = 13$ TeV collected with the ATLAS detector*, *Eur. Phys. J. C* **82** (2022) 95 [arXiv:2109.10627] [INSPIRE].

JHEP11(2024)047

[80] ATLAS collaboration, *Calibration of the light-flavour jet mistagging efficiency of the b-tagging algorithms with Z+jets events using 139 fb^{-1} of ATLAS proton–proton collision data at* $\sqrt{s} = 13$ *TeV*, *Eur. Phys. J. C* **83** (2023) 728 [arXiv:2301.06319] [INSPIRE].

[81] ATLAS collaboration, *Evidence for the $H \to b\bar{b}$ decay with the ATLAS detector*, *JHEP* **12** (2017) 024 [arXiv:1708.03299] [INSPIRE].

[82] P. Baldi et al., *Parameterized neural networks for high-energy physics*, *Eur. Phys. J. C* **76** (2016) 235 [arXiv:1601.07913] [INSPIRE].

[83] F. Chollet et al., *Keras*, https://keras.io, (2015).

[84] M. Abadi et al., *TensorFlow: Large-Scale Machine Learning on Heterogeneous Distributed Systems*, arXiv:1603.04467.

[85] R. Garnett, *Bayesian Optimization*, Cambridge University Press (2023).

[86] D.P. Kingma and J. Ba, *Adam: A Method for Stochastic Optimization*, arXiv:1412.6980 [INSPIRE].

[87] A.D. Bukin, *Fitting function for asymmetric peaks*, arXiv:0711.4449 [INSPIRE].

[88] B.N. Delaunay, *Sur la sphère vide*, *Bull. Acad. Sci. URSS* **1934** (1934) 793.

[89] ATLAS collaboration, *Measurement of the production cross section of pairs of isolated photons in pp collisions at 13 TeV with the ATLAS detector*, *JHEP* **11** (2021) 169 [arXiv:2107.09330] [INSPIRE].

[90] M. Bahr et al., *Herwig++ Physics and Manual*, *Eur. Phys. J. C* **58** (2008) 639 [arXiv:0803.0883] [INSPIRE].

[91] J. Bellm et al., *Herwig 7.0/Herwig++ 3.0 release note*, *Eur. Phys. J. C* **76** (2016) 196 [arXiv:1512.01178] [INSPIRE].

[92] ATLAS collaboration, *Measurements of inclusive and differential fiducial cross-sections of $t\bar{t}$ production with additional heavy-flavour jets in proton-proton collisions at* $\sqrt{s} = 13$ *TeV with the ATLAS detector*, *JHEP* **04** (2019) 046 [arXiv:1811.12113] [INSPIRE].

[93] ATLAS collaboration, *Study of heavy-flavor quarks produced in association with top-quark pairs at* $\sqrt{s} = 7$ *TeV using the ATLAS detector*, *Phys. Rev. D* **89** (2014) 072012 [arXiv:1304.6386] [INSPIRE].

[94] ATLAS collaboration, *Measurement of the cross-section for W boson production in association with b-jets in pp collisions at* $\sqrt{s} = 7$ *TeV with the ATLAS detector*, *JHEP* **06** (2013) 084 [arXiv:1302.2929] [INSPIRE].

[95] G. Cowan, K. Cranmer, E. Gross and O. Vitells, *Asymptotic formulae for likelihood-based tests of new physics*, *Eur. Phys. J. C* **71** (2011) 1554 [*Erratum ibid.* **73** (2013) 2501] [arXiv:1007.1727] [INSPIRE].

[96] A.L. Read, *Presentation of search results: The CL_s technique*, *J. Phys. G* **28** (2002) 2693 [INSPIRE].

[97] E. Gross and O. Vitells, *Trial factors for the look elsewhere effect in high energy physics*, *Eur. Phys. J. C* **70** (2010) 525 [arXiv:1005.1891] [INSPIRE].

[98] ATLAS collaboration, *ATLAS Computing Acknowledgements*, ATL-SOFT-PUB-2023-001, CERN, Geneva (2023).

JHEP11(2024)047

The ATLAS collaboration

G. Aad[103], E. Aakvaag[16], B. Abbott[121], K. Abeling[55], N.J. Abicht[49], S.H. Abidi[29], M. Aboelela[44], A. Aboulhorma[35e], H. Abramowicz[152], H. Abreu[151], Y. Abulaiti[118], B.S. Acharya[69a,69b,l], A. Ackermann[63a], C. Adam Bourdarios[4], L. Adamczyk[86a], S.V. Addepalli[26], M.J. Addison[102], J. Adelman[116], A. Adiguzel[21c], T. Adye[135], A.A. Affolder[137], Y. Afik[39], M.N. Agaras[13], J. Agarwala[73a,73b], A. Aggarwal[101], C. Agheorghiesei[27c], A. Ahmad[36], F. Ahmadov[38,z], W.S. Ahmed[105], S. Ahuja[96], X. Ai[62e], G. Aielli[76a,76b], A. Aikot[164], M. Ait Tamlihat[35e], B. Aitbenchikh[35a], I. Aizenberg[170], M. Akbiyik[101], T.P.A. Åkesson[99], A.V. Akimov[37], D. Akiyama[169], N.N. Akolkar[24], S. Aktas[21a], K. Al Khoury[41], G.L. Alberghi[23b], J. Albert[166], P. Albicocco[53], G.L. Albouy[60], S. Alderweireldt[52], Z.L. Alegria[122], M. Aleksa[36], I.N. Aleksandrov[38], C. Alexa[27b], T. Alexopoulos[10], F. Alfonsi[23b], M. Algren[56], M. Alhroob[142], B. Ali[133], H.M.J. Ali[92], S. Ali[149], S.W. Alibocus[93], M. Aliev[33c], G. Alimonti[71a], W. Alkakhi[55], C. Allaire[66], B.M.M. Allbrooke[147], J.F. Allen[52], C.A. Allendes Flores[138f], P.P. Allport[20], A. Aloisio[72a,72b], F. Alonso[91], C. Alpigiani[139], M. Alvarez Estevez[100], A. Alvarez Fernandez[101], M. Alves Cardoso[56], M.G. Alviggi[72a,72b], M. Aly[102], Y. Amaral Coutinho[83b], A. Ambler[105], C. Amelung[36], M. Amerl[102], C.G. Ames[110], D. Amidei[107], K.J. Amirie[156], S.P. Amor Dos Santos[131a], K.R. Amos[164], V. Ananiev[126], C. Anastopoulos[140], T. Andeen[11], J.K. Anders[36], S.Y. Andrean[47a,47b], A. Andreazza[71a,71b], S. Angelidakis[9], A. Angerami[41,ab], A.V. Anisenkov[37], A. Annovi[74a], C. Antel[56], M.T. Anthony[140], E. Antipov[146], M. Antonelli[53], F. Anulli[75a], M. Aoki[84], T. Aoki[154], J.A. Aparisi Pozo[164], M.A. Aparo[147], L. Aperio Bella[48], C. Appelt[18], A. Apyan[26], S.J. Arbiol Val[87], C. Arcangeletti[53], A.T.H. Arce[51], E. Arena[93], J-F. Arguin[109], S. Argyropoulos[54], J.-H. Arling[48], O. Arnaez[4], H. Arnold[115], G. Artoni[75a,75b], H. Asada[112], K. Asai[119], S. Asai[154], N.A. Asbah[36], K. Assamagan[29], R. Astalos[28a], S. Atashi[160], R.J. Atkin[33a], M. Atkinson[163], H. Atmani[35f], P.A. Atmasiddha[129], K. Augsten[133], S. Auricchio[72a,72b], A.D. Auriol[20], V.A. Austrup[102], G. Avolio[36], K. Axiotis[56], G. Azuelos[109,af], D. Babal[28b], H. Bachacou[136], K. Bachas[153,p], A. Bachiu[34], F. Backman[47a,47b], A. Badea[39], T.M. Baer[107], P. Bagnaia[75a,75b], M. Bahmani[18], D. Bahner[54], K. Bai[124], A.J. Bailey[164], J.T. Baines[135], L. Baines[95], O.K. Baker[173], E. Bakos[15], D. Bakshi Gupta[8], V. Balakrishnan[121], R. Balasubramanian[115], E.M. Baldin[37], P. Balek[86a], E. Ballabene[23b,23a], F. Balli[136], L.M. Baltes[63a], W.K. Balunas[32], J. Balz[101], E. Banas[87], M. Bandieramonte[130], A. Bandyopadhyay[24], S. Bansal[24], L. Barak[152], M. Barakat[48], E.L. Barberio[106], D. Barberis[57b,57a], M. Barbero[103], M.Z. Barel[115], K.N. Barends[33a], T. Barillari[111], M-S. Barisits[36], T. Barklow[144], P. Baron[123], D.A. Baron Moreno[102], A. Baroncelli[62a], G. Barone[29], A.J. Barr[127], J.D. Barr[97], F. Barreiro[100], J. Barreiro Guimarães da Costa[14a], U. Barron[152], M.G. Barros Teixeira[131a], S. Barsov[37], F. Bartels[63a], R. Bartoldus[144], A.E. Barton[92], P. Bartos[28a], A. Basan[101], M. Baselga[49], A. Bassalat[66,b], M.J. Basso[157a], R.L. Bates[59], S. Batlamous[35e], B. Batool[142], M. Battaglia[137], D. Battulga[18], M. Bauce[75a,75b], M. Bauer[36], P. Bauer[24], L.T. Bazzano Hurrell[30], J.B. Beacham[51], T. Beau[128], J.Y. Beaucamp[91], P.H. Beauchemin[159], P. Bechtle[24], H.P. Beck[19,o], K. Becker[168], A.J. Beddall[82], V.A. Bednyakov[38], C.P. Bee[146], L.J. Beemster[15],

JHEP11(2024)047

T.A. Beermann[36], M. Begalli[83d], M. Begel[29], A. Behera[146], J.K. Behr[48], J.F. Beirer[36], F. Beisiegel[24], M. Belfkir[117b], G. Bella[152], L. Bellagamba[23b], A. Bellerive[34], P. Bellos[20], K. Beloborodov[37], D. Benchekroun[35a], F. Bendebba[35a], Y. Benhammou[152], K.C. Benkendorfer[61], L. Beresford[48], M. Beretta[53], E. Bergeaas Kuutmann[162], N. Berger[4], B. Bergmann[133], J. Beringer[17a], G. Bernardi[5], C. Bernius[144], F.U. Bernlochner[24], F. Bernon[36,103], A. Berrocal Guardia[13], T. Berry[96], P. Berta[134], A. Berthold[50], S. Bethke[111], A. Betti[75a,75b], A.J. Bevan[95], N.K. Bhalla[54], M. Bhamjee[33c], S. Bhatta[146], D.S. Bhattacharya[167], P. Bhattarai[144], K.D. Bhide[54], V.S. Bhopatkar[122], R.M. Bianchi[130], G. Bianco[23b,23a], O. Biebel[110], R. Bielski[124], M. Biglietti[77a], C.S. Billingsley[44], M. Bindi[55], A. Bingul[21b], C. Bini[75a,75b], A. Biondini[93], C.J. Birch-sykes[102], G.A. Bird[32], M. Birman[170], M. Biros[134], S. Biryukov[147], T. Bisanz[49], E. Bisceglie[43b,43a], J.P. Biswal[135], D. Biswas[142], K. Bjørke[126], I. Bloch[48], A. Blue[59], U. Blumenschein[95], J. Blumenthal[101], V.S. Bobrovnikov[37], M. Boehler[54], B. Boehm[167], D. Bogavac[36], A.G. Bogdanchikov[37], C. Bohm[47a], V. Boisvert[96], P. Bokan[36], T. Bold[86a], M. Bomben[5], M. Bona[95], M. Boonekamp[136], C.D. Booth[96], A.G. Borbély[59], I.S. Bordulev[37], H.M. Borecka-Bielska[109], G. Borissov[92], D. Bortoletto[127], D. Boscherini[23b], M. Bosman[13], J.D. Bossio Sola[36], K. Bouaouda[35a], N. Bouchhar[164], J. Boudreau[130], E.V. Bouhova-Thacker[92], D. Boumediene[40], R. Bouquet[57b,57a], A. Boveia[120], J. Boyd[36], D. Boye[29], I.R. Boyko[38], J. Bracinik[20], N. Brahimi[4], G. Brandt[172], O. Brandt[32], F. Braren[48], B. Brau[104], J.E. Brau[124], R. Brener[170], L. Brenner[115], R. Brenner[162], S. Bressler[170], D. Britton[59], D. Britzger[111], I. Brock[24], R. Brock[108], G. Brooijmans[41], E. Brost[29], L.M. Brown[166], L.E. Bruce[61], T.L. Bruckler[127], P.A. Bruckman de Renstrom[87], B. Brüers[48], A. Bruni[23b], G. Bruni[23b], D. Brunner[47b], M. Bruschi[23b], N. Bruscino[75a,75b], T. Buanes[16], Q. Buat[139], D. Buchin[111], A.G. Buckley[59], O. Bulekov[37], B.A. Bullard[144], S. Burdin[93], C.D. Burgard[49], A.M. Burger[36], B. Burghgrave[8], O. Burlayenko[54], J.T.P. Burr[32], C.D. Burton[11], J.C. Burzynski[143], E.L. Busch[41], V. Büscher[101], P.J. Bussey[59], J.M. Butler[25], C.M. Buttar[59], J.M. Butterworth[97], W. Buttinger[135], C.J. Buxo Vazquez[108], A.R. Buzykaev[37], S. Cabrera Urbán[164], L. Cadamuro[66], D. Caforio[58], H. Cai[130], Y. Cai[14a,14e], Y. Cai[14c], V.M.M. Cairo[36], O. Cakir[3a], N. Calace[36], P. Calafiura[17a], G. Calderini[128], P. Calfayan[68], G. Callea[59], L.P. Caloba[83b], D. Calvet[40], S. Calvet[40], M. Calvetti[74a,74b], R. Camacho Toro[128], S. Camarda[36], D. Camarero Munoz[26], P. Camarri[76a,76b], M.T. Camerlingo[72a,72b], D. Cameron[36], C. Camincher[166], M. Campanelli[97], A. Camplani[42], V. Canale[72a,72b], A.C. Canbay[3a], J. Cantero[164], Y. Cao[163], F. Capocasa[26], M. Capua[43b,43a], A. Carbone[71a,71b], R. Cardarelli[76a], J.C.J. Cardenas[8], F. Cardillo[164], G. Carducci[43b,43a], T. Carli[36], G. Carlino[72a], J.I. Carlotto[13], B.T. Carlson[130,q], E.M. Carlson[166,157a], L. Carminati[71a,71b], A. Carnelli[136], M. Carnesale[75a,75b], S. Caron[114], E. Carquin[138f], S. Carrá[71a], G. Carratta[23b,23a], A.M. Carroll[124], T.M. Carter[52], M.P. Casado[13,i], M. Caspar[48], F.L. Castillo[4], L. Castillo Garcia[13], V. Castillo Gimenez[164], N.F. Castro[131a,131e], A. Catinaccio[36], J.R. Catmore[126], T. Cavaliere[4], V. Cavaliere[29], N. Cavalli[23b,23a], Y.C. Cekmecelioglu[48], E. Celebi[21a], S. Cella[36], F. Celli[127], M.S. Centonze[70a,70b], V. Cepaitis[56], K. Cerny[123], A.S. Cerqueira[83a], A. Cerri[147], L. Cerrito[76a,76b], F. Cerutti[17a], B. Cervato[142], A. Cervelli[23b], G. Cesarini[53], S.A. Cetin[82],

D. Chakraborty[116], J. Chan[17a], W.Y. Chan[154], J.D. Chapman[32], E. Chapon[136], B. Chargeishvili[150b], D.G. Charlton[20], M. Chatterjee[19], C. Chauhan[134], Y. Che[14c], S. Chekanov[6], S.V. Chekulaev[157a], G.A. Chelkov[38,a], A. Chen[107], B. Chen[152], B. Chen[166], H. Chen[14c], H. Chen[29], J. Chen[62c], J. Chen[143], M. Chen[127], S. Chen[154], S.J. Chen[14c], X. Chen[62c,136], X. Chen[14b,ae], Y. Chen[62a], C.L. Cheng[171], H.C. Cheng[64a], S. Cheong[144], A. Cheplakov[38], E. Cheremushkina[48], E. Cherepanova[115], R. Cherkaoui El Moursli[35e], E. Cheu[7], K. Cheung[65], L. Chevalier[136], V. Chiarella[53], G. Chiarelli[74a], N. Chiedde[103], G. Chiodini[70a], A.S. Chisholm[20], A. Chitan[27b], M. Chitishvili[164], M.V. Chizhov[38,r], K. Choi[11], Y. Chou[139], E.Y.S. Chow[114], K.L. Chu[170], M.C. Chu[64a], X. Chu[14a,14e], J. Chudoba[132], J.J. Chwastowski[87], D. Cieri[111], K.M. Ciesla[86a], V. Cindro[94], A. Ciocio[17a], F. Cirotto[72a,72b], Z.H. Citron[170], M. Citterio[71a], D.A. Ciubotaru[27b], A. Clark[56], P.J. Clark[52], C. Clarry[156], J.M. Clavijo Columbie[48], S.E. Clawson[48], C. Clement[47a,47b], J. Clercx[48], Y. Coadou[103], M. Cobal[69a,69c], A. Coccaro[57b], R.F. Coelho Barrue[131a], R. Coelho Lopes De Sa[104], S. Coelli[71a], B. Cole[41], J. Collot[60], P. Conde Muiño[131a,131g], M.P. Connell[33c], S.H. Connell[33c], E.I. Conroy[127], F. Conventi[72a,ag], H.G. Cooke[20], A.M. Cooper-Sarkar[127], A. Cordeiro Oudot Choi[128], L.D. Corpe[40], M. Corradi[75a,75b], F. Corriveau[105,x], A. Cortes-Gonzalez[18], M.J. Costa[164], F. Costanza[4], D. Costanzo[140], B.M. Cote[120], G. Cowan[96], K. Cranmer[171], D. Cremonini[23b,23a], S. Crépé-Renaudin[60], F. Crescioli[128], M. Cristinziani[142], M. Cristoforetti[78a,78b], V. Croft[115], J.E. Crosby[122], G. Crosetti[43b,43a], A. Cueto[100], T. Cuhadar Donszelmann[160], H. Cui[14a,14e], Z. Cui[7], W.R. Cunningham[59], F. Curcio[164], J.R. Curran[52], P. Czodrowski[36], M.M. Czurylo[36], M.J. Da Cunha Sargedas De Sousa[57b,57a], J.V. Da Fonseca Pinto[83b], C. Da Via[102], W. Dabrowski[86a], T. Dado[49], S. Dahbi[149], T. Dai[107], D. Dal Santo[19], C. Dallapiccola[104], M. Dam[42], G. D'amen[29], V. D'Amico[110], J. Damp[101], J.R. Dandoy[34], M. Danninger[143], V. Dao[36], G. Darbo[57b], S. Darmora[6], S.J. Das[29,ah], S. D'Auria[71a,71b], A. D'Avanzo[131a], C. David[33a], T. Davidek[134], B. Davis-Purcell[34], I. Dawson[95], H.A. Day-hall[133], K. De[8], R. De Asmundis[72a], N. De Biase[48], S. De Castro[23b,23a], N. De Groot[114], P. de Jong[115], H. De la Torre[116], A. De Maria[14c], A. De Salvo[75a], U. De Sanctis[76a,76b], F. De Santis[70a,70b], A. De Santo[147], J.B. De Vivie De Regie[60], D.V. Dedovich[38], J. Degens[115], A.M. Deiana[44], F. Del Corso[23b,23a], J. Del Peso[100], F. Del Rio[63a], L. Delagrange[128], F. Deliot[136], C.M. Delitzsch[49], M. Della Pietra[72a,72b], D. Della Volpe[56], A. Dell'Acqua[36], L. Dell'Asta[71a,71b], M. Delmastro[4], P.A. Delsart[60], S. Demers[173], M. Demichev[38], S.P. Denisov[37], L. D'Eramo[40], D. Derendarz[87], F. Derue[128], P. Dervan[93], K. Desch[24], C. Deutsch[24], F.A. Di Bello[57b,57a], A. Di Ciaccio[76a,76b], L. Di Ciaccio[4], A. Di Domenico[75a,75b], C. Di Donato[72a,72b], A. Di Girolamo[36], G. Di Gregorio[36], A. Di Luca[78a,78b], B. Di Micco[77a,77b], R. Di Nardo[77a,77b], M. Diamantopoulou[34], F.A. Dias[115], T. Dias Do Vale[143], M.A. Diaz[138a,138b], F.G. Diaz Capriles[24], M. Didenko[164], E.B. Diehl[107], S. Díez Cornell[48], C. Diez Pardos[142], C. Dimitriadi[162,24], A. Dimitrievska[17a], J. Dingfelder[24], I-M. Dinu[27b], S.J. Dittmeier[63b], F. Dittus[36], M. Divisek[134], F. Djama[103], T. Djobava[150b], C. Doglioni[102,99], A. Dohnalova[28a], J. Dolejsi[134], Z. Dolezal[134], K.M. Dona[39], M. Donadelli[83c], B. Dong[108], J. Donini[40], A. D'Onofrio[72a,72b], M. D'Onofrio[93], J. Dopke[135], A. Doria[72a],

JHEP11(2024)047

N. Dos Santos Fernandes[131a], P. Dougan[102], M.T. Dova[91], A.T. Doyle[59], M.A. Draguet[127], E. Dreyer[170], I. Drivas-koulouris[10], M. Drnevich[118], M. Drozdova[56], D. Du[62a], T.A. du Pree[115], F. Dubinin[37], M. Dubovsky[28a], E. Duchovni[170], G. Duckeck[110], O.A. Ducu[27b], D. Duda[52], A. Dudarev[36], E.R. Duden[26], M. D'uffizi[102], L. Duflot[66], M. Dührssen[36], A.E. Dumitriu[27b], M. Dunford[63a], S. Dungs[49], K. Dunne[47a,47b], A. Duperrin[103], H. Duran Yildiz[3a], M. Düren[58], A. Durglishvili[150b], B.L. Dwyer[116], G.I. Dyckes[17a], M. Dyndal[86a], B.S. Dziedzic[87], Z.O. Earnshaw[147], G.H. Eberwein[127], B. Eckerova[28a], S. Eggebrecht[55], E. Egidio Purcino De Souza[128], L.F. Ehrke[56], G. Eigen[16], K. Einsweiler[17a], T. Ekelof[162], P.A. Ekman[99], S. El Farkh[35b], Y. El Ghazali[35b], H. El Jarrari[36], A. El Moussaouy[109], V. Ellajosyula[162], M. Ellert[162], F. Ellinghaus[172], N. Ellis[36], J. Elmsheuser[29], M. Elsing[36], D. Emeliyanov[135], Y. Enari[154], I. Ene[17a], S. Epari[13], P.A. Erland[87], M. Errenst[172], M. Escalier[66], C. Escobar[164], E. Etzion[152], G. Evans[131a], H. Evans[68], L.S. Evans[96], A. Ezhilov[37], S. Ezzarqtouni[35a], F. Fabbri[23b,23a], L. Fabbri[23b,23a], G. Facini[97], V. Fadeyev[137], R.M. Fakhrutdinov[37], D. Fakoudis[101], S. Falciano[75a], L.F. Falda Ulhoa Coelho[36], P.J. Falke[24], J. Faltova[134], C. Fan[163], Y. Fan[14a], Y. Fang[14a,14e], M. Fanti[71a,71b], M. Faraj[69a,69b], Z. Farazpay[98], A. Farbin[8], A. Farilla[77a], T. Farooque[108], S.M. Farrington[52], F. Fassi[35e], D. Fassouliotis[9], M. Faucci Giannelli[76a,76b], W.J. Fawcett[32], L. Fayard[66], P. Federic[134], P. Federicova[132], O.L. Fedin[37,a], M. Feickert[171], L. Feligioni[103], D.E. Fellers[124], C. Feng[62b], M. Feng[14b], Z. Feng[115], M.J. Fenton[160], L. Ferencz[48], R.A.M. Ferguson[92], S.I. Fernandez Luengo[138f], P. Fernandez Martinez[13], M.J.V. Fernoux[103], J. Ferrando[92], A. Ferrari[162], P. Ferrari[115,114], R. Ferrari[73a], D. Ferrere[56], C. Ferretti[107], F. Fiedler[101], P. Fiedler[133], A. Filipčič[94], E.K. Filmer[1], F. Filthaut[114], M.C.N. Fiolhais[131a,131c,c], L. Fiorini[164], W.C. Fisher[108], T. Fitschen[102], P.M. Fitzhugh[136], I. Fleck[142], P. Fleischmann[107], T. Flick[172], M. Flores[33d,ac], L.R. Flores Castillo[64a], L. Flores Sanz De Acedo[36], F.M. Follega[78a,78b], N. Fomin[16], J.H. Foo[156], A. Formica[136], A.C. Forti[102], E. Fortin[36], A.W. Fortman[17a], M.G. Foti[17a], L. Fountas[9,j], D. Fournier[66], H. Fox[92], P. Francavilla[74a,74b], S. Francescato[61], S. Franchellucci[56], M. Franchini[23b,23a], S. Franchino[63a], D. Francis[36], L. Franco[114], V. Franco Lima[36], L. Franconi[48], M. Franklin[61], G. Frattari[26], W.S. Freund[83b], Y.Y. Frid[152], J. Friend[59], N. Fritzsche[50], A. Froch[54], D. Froidevaux[36], J.A. Frost[127], Y. Fu[62a], S. Fuenzalida Garrido[138f], M. Fujimoto[103], K.Y. Fung[64a], E. Furtado De Simas Filho[83e], M. Furukawa[154], J. Fuster[164], A. Gabrielli[23b,23a], A. Gabrielli[156], P. Gadow[36], G. Gagliardi[57b,57a], L.G. Gagnon[17a], S. Galantzan[152], E.J. Gallas[127], B.J. Gallop[135], K.K. Gan[120], S. Ganguly[154], Y. Gao[52], F.M. Garay Walls[138a,138b], B. Garcia[29], C. García[164], A. Garcia Alonso[115], A.G. Garcia Caffaro[173], J.E. García Navarro[164], M. Garcia-Sciveres[17a], G.L. Gardner[129], R.W. Gardner[39], N. Garelli[159], D. Garg[80], R.B. Garg[144,m], J.M. Gargan[52], C.A. Garner[156], C.M. Garvey[33a], P. Gaspar[83b], V.K. Gassmann[159], G. Gaudio[73a], V. Gautam[13], P. Gauzzi[75a,75b], I.L. Gavrilenko[37], A. Gavrilyuk[37], C. Gay[165], G. Gaycken[48], E.N. Gazis[10], A.A. Geanta[27b], C.M. Gee[137], A. Gekow[120], C. Gemme[57b], M.H. Genest[60], A.D. Gentry[113], S. George[96], W.F. George[20], T. Geralis[46], P. Gessinger-Befurt[36], M.E. Geyik[172], M. Ghani[168], M. Ghneimat[142], K. Ghorbanian[95], A. Ghosal[142], A. Ghosh[160], A. Ghosh[7], B. Giacobbe[23b],

S. Giagu[75a,75b], T. Giani[115], P. Giannetti[74a], A. Giannini[62a], S.M. Gibson[96], M. Gignac[137], D.T. Gil[86b], A.K. Gilbert[86a], B.J. Gilbert[41], D. Gillberg[34], G. Gilles[115], L. Ginabat[128], D.M. Gingrich[2,af], M.P. Giordani[69a,69c], P.F. Giraud[136], G. Giugliarelli[69a,69c], D. Giugni[71a], F. Giuli[36], I. Gkialas[9,j], L.K. Gladilin[37], C. Glasman[100], G.R. Gledhill[124], G. Glemža[48], M. Glisic[124], I. Gnesi[43b,f], Y. Go[29], M. Goblirsch-Kolb[36], B. Gocke[49], D. Godin[109], B. Gokturk[21a], S. Goldfarb[106], T. Golling[56], M.G.D. Gololo[33g], D. Golubkov[37], J.P. Gombas[108], A. Gomes[131a,131b], G. Gomes Da Silva[142], A.J. Gomez Delegido[164], R. Gonçalo[131a,131c], L. Gonella[20], A. Gongadze[150c], F. Gonnella[20], J.L. Gonski[144], R.Y. González Andana[52], S. González de la Hoz[164], R. Gonzalez Lopez[93], C. Gonzalez Renteria[17a], M.V. Gonzalez Rodrigues[48], R. Gonzalez Suarez[162], S. Gonzalez-Sevilla[56], L. Goossens[36], B. Gorini[36], E. Gorini[70a,70b], A. Gorišek[94], T.C. Gosart[129], A.T. Goshaw[51], M.I. Gostkin[38], S. Goswami[122], C.A. Gottardo[36], S.A. Gotz[110], M. Gouighri[35b], V. Goumarre[48], A.G. Goussiou[139], N. Govender[33c], I. Grabowska-Bold[86a], K. Graham[34], E. Gramstad[126], S. Grancagnolo[70a,70b], C.M. Grant[1,136], P.M. Gravila[27f], F.G. Gravili[70a,70b], H.M. Gray[17a], M. Greco[70a,70b], C. Grefe[24], I.M. Gregor[48], P. Grenier[144], S.G. Grewe[111], A.A. Grillo[137], K. Grimm[31], S. Grinstein[13,t], J.-F. Grivaz[66], E. Gross[170], J. Grosse-Knetter[55], J.C. Grundy[127], L. Guan[107], C. Gubbels[165], J.G.R. Guerrero Rojas[164], G. Guerrieri[69a,69c], F. Guescini[111], R. Gugel[101], J.A.M. Guhit[107], A. Guida[18], E. Guilloton[168], S. Guindon[36], F. Guo[14a,14e], J. Guo[62c], L. Guo[48], Y. Guo[107], R. Gupta[48], R. Gupta[130], S. Gurbuz[24], S.S. Gurdasani[54], G. Gustavino[36], M. Guth[56], P. Gutierrez[121], L.F. Gutierrez Zagazeta[129], M. Gutsche[50], C. Gutschow[97], C. Gwenlan[127], C.B. Gwilliam[93], E.S. Haaland[126], A. Haas[118], M. Habedank[48], C. Haber[17a], H.K. Hadavand[8], A. Hadef[50], S. Hadzic[111], A.I. Hagan[92], J.J. Hahn[142], E.H. Haines[97], M. Haleem[167], J. Haley[122], J.J. Hall[140], G.D. Hallewell[103], L. Halser[19], K. Hamano[166], M. Hamer[24], G.N. Hamity[52], E.J. Hampshire[96], J. Han[62b], K. Han[62a], L. Han[14c], L. Han[62a], S. Han[17a], Y.F. Han[156], K. Hanagaki[84], M. Hance[137], D.A. Hangal[41], H. Hanif[143], M.D. Hank[129], J.B. Hansen[42], P.H. Hansen[42], K. Hara[158], D. Harada[56], T. Harenberg[172], S. Harkusha[37], M.L. Harris[104], Y.T. Harris[127], J. Harrison[13], N.M. Harrison[120], P.F. Harrison[168], N.M. Hartman[111], N.M. Hartmann[110], Y. Hasegawa[141], R. Hauser[108], C.M. Hawkes[20], R.J. Hawkings[36], Y. Hayashi[154], S. Hayashida[112], D. Hayden[108], C. Hayes[107], R.L. Hayes[115], C.P. Hays[127], J.M. Hays[95], H.S. Hayward[93], F. He[62a], M. He[14a,14e], Y. He[155], Y. He[48], Y. He[97], N.B. Heatley[95], V. Hedberg[99], A.L. Heggelund[126], N.D. Hehir[95,*], C. Heidegger[54], K.K. Heidegger[54], W.D. Heidorn[81], J. Heilman[34], S. Heim[48], T. Heim[17a], J.G. Heinlein[129], J.J. Heinrich[124], L. Heinrich[111,ad], J. Hejbal[132], A. Held[171], S. Hellesund[16], C.M. Helling[165], S. Hellman[47a,47b], R.C.W. Henderson[92], L. Henkelmann[32], A.M. Henriques Correia[36], H. Herde[99], Y. Hernández Jiménez[146], L.M. Herrmann[24], T. Herrmann[50], G. Herten[54], R. Hertenberger[110], L. Hervas[36], M.E. Hesping[101], N.P. Hessey[157a], E. Hill[156], S.J. Hillier[20], J.R. Hinds[108], F. Hinterkeuser[24], M. Hirose[125], S. Hirose[158], D. Hirschbuehl[172], T.G. Hitchings[102], B. Hiti[94], J. Hobbs[146], R. Hobincu[27e], N. Hod[170], M.C. Hodgkinson[140], B.H. Hodkinson[127], A. Hoecker[36], D.D. Hofer[107], J. Hofer[48], T. Holm[24], M. Holzbock[111], L.B.A.H. Hommels[32], B.P. Honan [102], J. Hong [62c], T.M. Hong [130], B.H. Hooberman [163], W.H. Hopkins [6], Y. Horii [112], S. Hou [149], A.S. Howard [94], J. Howarth [59], J. Hoya [6], M. Hrabovsky [123], A. Hrynevich [48], T. Hryn'ova [4], P.J. Hsu [65], S.-C. Hsu [139], Q. Hu [62a], S. Huang [64b], X. Huang [14a,14e], Y. Huang [140], Y. Huang [14a], Z. Huang [102], Z. Hubacek [133], M. Huebner [24], F. Huegging [24], T.B. Huffman [127], C.A. Hugli [48], M. Huhtinen [36], S.K. Huiberts [16], R. Hulsken [105], N. Huseynov [12], J. Huston [108], J. Huth [61], R. Hyneman [144], G. Iacobucci [56], G. Iakovidis [29], I. Ibragimov [142], L. Iconomidou-Fayard [66], J.P. Iddon [36], P. Iengo [72a,72b], R. Iguchi [154], T. Iizawa [127], Y. Ikegami [84], N. Ilic [156], H. Imam [35a], M. Ince Lezki [56], T. Ingebretsen Carlson [47a,47b], G. Introzzi [73a,73b], M. Iodice [77a], V. Ippolito [75a,75b], R.K. Irwin [93], M. Ishino [154], W. Islam [171], C. Issever [18,48], S. Istin [21a,aj], H. Ito [169], R. Iuppa [78a,78b], A. Ivina [170], J.M. Izen [45], V. Izzo [72a], P. Jacka [132,133], P. Jackson [1], B.P. Jaeger [143], C.S. Jagfeld [110], G. Jain [157a], P. Jain [54], K. Jakobs [54], T. Jakoubek [170], J. Jamieson [59], K.W. Janas [86a], M. Javurkova [104], L. Jeanty [124], J. Jejelava [150a,aa], P. Jenni [54,g], C.E. Jessiman [34], C. Jia [62b], J. Jia [146], X. Jia [61], X. Jia [14a,14e], Z. Jia [14c], S. Jiggins [48], J. Jimenez Pena [13], S. Jin [14c], A. Jinaru [27b], O. Jinnouchi [155], P. Johansson [140], K.A. Johns [7], J.W. Johnson [137], D.M. Jones [32], E. Jones [48], P. Jones [32], R.W.L. Jones [92], T.J. Jones [93], H.L. Joos [55,36], R. Joshi [120], J. Jovicevic [15], X. Ju [17a], J.J. Junggeburth [104], T. Junkermann [63a], A. Juste Rozas [13,t], M.K. Juzek [87], S. Kabana [138e], A. Kaczmarska [87], M. Kado [111], H. Kagan [120], M. Kagan [144], A. Kahn [41], A. Kahn [129], C. Kahra [101], T. Kaji [154], E. Kajomovitz [151], N. Kakati [170], I. Kalaitzidou [54], C.W. Kalderon [29], N.J. Kang [137], D. Kar [33g], K. Karava [127], M.J. Kareem [157b], E. Karentzos [54], I. Karkanias [153], O. Karkout [115], S.N. Karpov [38], Z.M. Karpova [38], V. Kartvelishvili [92], A.N. Karyukhin [37], E. Kasimi [153], J. Katzy [48], S. Kaur [34], K. Kawade [141], M.P. Kawale [121], C. Kawamoto [88], T. Kawamoto [62a], E.F. Kay [36], F.I. Kaya [159], S. Kazakos [108], V.F. Kazanin [37], Y. Ke [146], J.M. Keaveney [33a], R. Keeler [166], G.V. Kehris [61], J.S. Keller [34], A.S. Kelly [97], J.J. Kempster [147], P.D. Kennedy [101], O. Kepka [132], B.P. Kerridge [135], S. Kersten [172], B.P. Kerševan [94], L. Keszeghova [28a], S. Ketabchi Haghighat [156], R.A. Khan [130], A. Khanov [122], A.G. Kharlamov [37], T. Kharlamova [37], E.E. Khoda [139], M. Kholodenko [37], T.J. Khoo [18], G. Khoriauli [167], J. Khubua [150b,*], Y.A.R. Khwaira [66], B. Kibirige [33g], A. Kilgallon [124], D.W. Kim [47a,47b], Y.K. Kim [39], N. Kimura [97], M.K. Kingston [55], A. Kirchhoff [55], C. Kirfel [24], F. Kirfel [24], J. Kirk [135], A.E. Kiryunin [111], C. Kitsaki [10], O. Kivernyk [24], M. Klassen [63a], C. Klein [34], L. Klein [167], M.H. Klein [44], S.B. Klein [56], U. Klein [93], P. Klimek [36], A. Klimentov [29], T. Klioutchnikova [36], P. Kluit [115], S. Kluth [111], E. Kneringer [79], T.M. Knight [156], A. Knue [49], R. Kobayashi [88], D. Kobylianskii [170], S.F. Koch [127], M. Kocian [144], P. Kodyš [134], D.M. Koeck [124], P.T. Koenig [24], T. Koffas [34], O. Kolay [50], I. Koletsou [4], T. Komarek [123], K. Köneke [54], A.X.Y. Kong [1], T. Kono [119], N. Konstantinidis [97], P. Kontaxakis [56], B. Konya [99], R. Kopeliansky [41], S. Koperny [86a], K. Korcyl [87], K. Kordas [153,e], A. Korn [97], S. Korn [55], I. Korolkov [13], N. Korotkova [37], B. Kortman [115], O. Kortner [111], S. Kortner [111], W.H. Kostecka [116], V.V. Kostyukhin [142], A. Kotsokechagia [136], A. Kotwal [51], A. Koulouris [36], A. Kourkoumeli-Charalampidi [73a,73b], C. Kourkoumelis [9], E. Kourlitis [111,ad], O. Kovanda [124], R. Kowalewski [166], W. Kozanecki [136], A.S. Kozhin [37], V.A. Kramarenko [37], G. Kramberger [94], P. Kramer [101], M.W. Krasny [128], A. Krasznahorkay [36], J.W. Kraus [172], J.A. Kremer [48],

T. Kresse[50], J. Kretzschmar[93], K. Kreul[18], P. Krieger[156], S. Krishnamurthy[104], M. Krivos[134], K. Krizka[20], K. Kroeninger[49], H. Kroha[111], J. Kroll[132], J. Kroll[129], K.S. Krowpman[108], U. Kruchonak[38], H. Krüger[24], N. Krumnack[81], M.C. Kruse[51], O. Kuchinskaia[37], S. Kuday[3a], S. Kuehn[36], R. Kuesters[54], T. Kuhl[48], V. Kukhtin[38], Y. Kulchitsky[37,a], S. Kuleshov[138d,138b], M. Kumar[33g], N. Kumari[48], P. Kumari[157b], A. Kupco[132], T. Kupfer[49], A. Kupich[37], O. Kuprash[54], H. Kurashige[85], L.L. Kurchaninov[157a], O. Kurdysh[66], Y.A. Kurochkin[37], A. Kurova[37], M. Kuze[155], A.K. Kvam[104], J. Kvita[123], T. Kwan[105], N.G. Kyriacou[107], L.A.O. Laatu[103], C. Lacasta[164], F. Lacava[75a,75b], H. Lacker[18], D. Lacour[128], N.N. Lad[97], E. Ladygin[38], A. Lafarge[40], B. Laforge[128], T. Lagouri[173], F.Z. Lahbabi[35a], S. Lai[55], I.K. Lakomiec[86a], N. Lalloue[60], J.E. Lambert[166], S. Lammers[68], W. Lampl[7], C. Lampoudis[153,e], G. Lamprinoudis[101], A.N. Lancaster[116], E. Lançon[29], U. Landgraf[54], M.P.J. Landon[95], V.S. Lang[54], O.K.B. Langrekken[126], A.J. Lankford[160], F. Lanni[36], K. Lantzsch[24], A. Lanza[73a], A. Lapertosa[57b,57a], J.F. Laporte[136], T. Lari[71a], F. Lasagni Manghi[23b], M. Lassnig[36], V. Latonova[132], A. Laudrain[101], A. Laurier[151], S.D. Lawlor[140], Z. Lawrence[102], R. Lazaridou[168], M. Lazzaroni[71a,71b], B. Le[102], E.M. Le Boulicaut[51], B. Leban[23b,23a], A. Lebedev[81], M. LeBlanc[102], F. Ledroit-Guillon[60], A.C.A. Lee[97], S.C. Lee[149], S. Lee[47a,47b], T.F. Lee[93], L.L. Leeuw[33c], H.P. Lefebvre[96], M. Lefebvre[166], C. Leggett[17a], G. Lehmann Miotto[36], M. Leigh[56], W.A. Leight[104], W. Leinonen[114], A. Leisos[153,s], M.A.L. Leite[83c], C.E. Leitgeb[18], R. Leitner[134], K.J.C. Leney[44], T. Lenz[24], S. Leone[74a], C. Leonidopoulos[52], A. Leopold[145], C. Leroy[109], R. Les[108], C.G. Lester[32], M. Levchenko[37], J. Levêque[4], L.J. Levinson[170], G. Levrini[23b,23a], M.P. Lewicki[87], D.J. Lewis[4], A. Li[5], B. Li[62b], C. Li[62a], C-Q. Li[111], H. Li[62a], H. Li[62b], H. Li[14c], H. Li[14b], H. Li[62b], J. Li[62c], K. Li[139], L. Li[62c], M. Li[14a,14e], Q.Y. Li[62a], S. Li[14a,14e], S. Li[62d,62c,d], T. Li[5], X. Li[105], Z. Li[127], Z. Li[154], Z. Li[14a,14e], S. Liang[14a,14e], Z. Liang[14a], M. Liberatore[136], B. Liberti[76a], K. Lie[64c], J. Lieber Marin[83b], H. Lien[68], K. Lin[108], R.E. Lindley[7], J.H. Lindon[2], E. Lipeles[129], A. Lipniacka[16], A. Lister[165], J.D. Little[4], B. Liu[14a], B.X. Liu[143], D. Liu[62d,62c], E.H.L. Liu[20], J.B. Liu[62a], J.K.K. Liu[32], K. Liu[62d], K. Liu[62d,62c], M. Liu[62a], M.Y. Liu[62a], P. Liu[14a], Q. Liu[62d,139,62c], X. Liu[62a], X. Liu[62b], Y. Liu[14d,14e], Y.L. Liu[62b], Y.W. Liu[62a], J. Llorente Merino[143], S.L. Lloyd[95], E.M. Lobodzinska[48], P. Loch[7], T. Lohse[18], K. Lohwasser[140], E. Loiacono[48], M. Lokajicek[132,*], J.D. Lomas[20], J.D. Long[163], I. Longarini[160], L. Longo[70a,70b], R. Longo[163], I. Lopez Paz[67], A. Lopez Solis[48], N. Lorenzo Martinez[4], A.M. Lory[110], G. Löschcke Centeno[147], O. Loseva[37], X. Lou[47a,47b], X. Lou[14a,14e], A. Lounis[66], P.A. Love[92], G. Lu[14a,14e], M. Lu[80], S. Lu[129], Y.J. Lu[65], H.J. Lubatti[139], C. Luci[75a,75b], F.L. Lucio Alves[14c], F. Luehring[68], I. Luise[146], O. Lukianchuk[66], O. Lundberg[145], B. Lund-Jensen[145,*], N.A. Luongo[6], M.S. Lutz[36], A.B. Lux[25], D. Lynn[29], R. Lysak[132], E. Lytken[99], V. Lyubushkin[38], T. Lyubushkina[38], M.M. Lyukova[146], H. Ma[29], K. Ma[62a], L.L. Ma[62b], W. Ma[62a], Y. Ma[122], D.M. Mac Donell[166], G. Maccarrone[53], J.C. MacDonald[101], P.C. Machado De Abreu Farias[83b], R. Madar[40], T. Madula[97], J. Maeda[85], T. Maeno[29], H. Maguire[140], V. Maiboroda[136], A. Maio[131a,131b,131d], K. Maj[86a], O. Majersky[48], S. Majewski[124], N. Makovec[66], V. Maksimovic[15], B. Malaescu[128], Pa. Malecki[87], V.P. Maleev[37], F. Malek[60,n], M. Mali[94], D. Malito[96], U. Mallik[80,*], S. Maltezos[10], S. Malyukov[38], J. Mamuzic[13], G. Mancini[53], M.N. Mancini[26], G. Manco[73a,73b], J.P. Mandalia[95], I. Mandić[94], L. Manhaes de Andrade Filho[83a], I.M. Maniatis[170], J. Manjarres Ramos[90], D.C. Mankad[170], A. Mann[110], S. Manzoni[36], L. Mao[62c], X. Mapekula[33c], A. Marantis[153,s], G. Marchiori[5], M. Marcisovsky[132], C. Marcon[71a], M. Marinescu[20], S. Marium[48], M. Marjanovic[121], M. Markovitch[66], E.J. Marshall[92], Z. Marshall[17a], S. Marti-Garcia[164], T.A. Martin[168], V.J. Martin[52], B. Martin dit Latour[16], L. Martinelli[75a,75b], M. Martinez[13,t], P. Martinez Agullo[164], V.I. Martinez Outschoorn[104], P. Martinez Suarez[13], S. Martin-Haugh[135], G. Martinovicova[134], V.S. Martoiu[27b], A.C. Martyniuk[97], A. Marzin[36], D. Mascione[78a,78b], L. Masetti[101], T. Mashimo[154], J. Masik[102], A.L. Maslennikov[37], P. Massarotti[72a,72b], P. Mastrandrea[74a,74b], A. Mastroberardino[43b,43a], T. Masubuchi[154], T. Mathisen[162], J. Matousek[134], N. Matsuzawa[154], J. Maurer[27b], A.J. Maury[66], B. Maček[94], D.A. Maximov[37], R. Mazini[149], I. Maznas[116], M. Mazza[108], S.M. Mazza[137], E. Mazzeo[71a,71b], C. Mc Ginn[29], J.P. Mc Gowan[166], S.P. Mc Kee[107], C.C. McCracken[165], E.F. McDonald[106], A.E. McDougall[115], J.A. Mcfayden[147], R.P. McGovern[129], G. Mchedlidze[150b], R.P. Mckenzie[33g], T.C. Mclachlan[48], D.J. Mclaughlin[97], S.J. McMahon[135], C.M. Mcpartland[93], R.A. McPherson[166,x], S. Mehlhase[110], A. Mehta[93], D. Melini[164], B.R. Mellado Garcia[33g], A.H. Melo[55], F. Meloni[48], A.M. Mendes Jacques Da Costa[102], H.Y. Meng[156], L. Meng[92], S. Menke[111], M. Mentink[36], E. Meoni[43b,43a], G. Mercado[116], C. Merlassino[69a,69c], L. Merola[72a,72b], C. Meroni[71a,71b], J. Metcalfe[6], A.S. Mete[6], C. Meyer[68], J-P. Meyer[136], R.P. Middleton[135], L. Mijović[52], G. Mikenberg[170], M. Mikestikova[132], M. Mikuž[94], H. Mildner[101], A. Milic[36], D.W. Miller[39], E.H. Miller[144], L.S. Miller[34], A. Milov[170], D.A. Milstead[47a,47b], T. Min[14c], A.A. Minaenko[37], I.A. Minashvili[150b], L. Mince[59], A.I. Mincer[118], B. Mindur[86a], M. Mineev[38], Y. Mino[88], L.M. Mir[13], M. Miralles Lopez[59], M. Mironova[17a], A. Mishima[154], M.C. Missio[114], A. Mitra[168], V.A. Mitsou[164], Y. Mitsumori[112], O. Miu[156], P.S. Miyagawa[95], T. Mkrtchyan[63a], M. Mlinarevic[97], T. Mlinarevic[97], M. Mlynarikova[36], S. Mobius[19], P. Mogg[110], M.H. Mohamed Farook[113], A.F. Mohammed[14a,14e], S. Mohapatra[41], G. Mokgatitswane[33g], L. Moleri[170], B. Mondal[142], S. Mondal[133], K. Mönig[48], E. Monnier[103], L. Monsonis Romero[164], J. Montejo Berlingen[13], M. Montella[120], F. Montereali[77a,77b], F. Monticelli[91], S. Monzani[69a,69c], N. Morange[66], A.L. Moreira De Carvalho[131a], M. Moreno Llácer[164], C. Moreno Martinez[56], P. Morettini[57b], S. Morgenstern[36], M. Morii[61], M. Morinaga[154], F. Morodei[75a,75b], L. Morvaj[36], P. Moschovakos[36], B. Moser[36], M. Mosidze[150b], T. Moskalets[54], P. Moskvitina[114], J. Moss[31,k], A. Moussa[35d], E.J.W. Moyse[104], O. Mtintsilana[33g], S. Muanza[103], J. Mueller[130], D. Muenstermann[92], R. Müller[19], G.A. Mullier[162], A.J. Mullin[32], J.J. Mullin[129], D.P. Mungo[156], D. Munoz Perez[164], F.J. Munoz Sanchez[102], M. Murin[102], W.J. Murray[168,135], M. Muškinja[94], C. Mwewa[29], A.G. Myagkov[37,a], A.J. Myers[8], G. Myers[107], M. Myska[133], B.P. Nachman[17a], O. Nackenhorst[49], K. Nagai[127], K. Nagano[84], J.L. Nagle[29,ah], E. Nagy[103], A.M. Nairz[36], Y. Nakahama[84], K. Nakamura[84], K. Nakkalil[5], H. Nanjo[125], R. Narayan[44], E.A. Narayanan[113], I. Naryshkin[37], M. Naseri[34], S. Nasri[117b], C. Nass[24], G. Navarro[22a],

J. Navarro-Gonzalez[164], R. Nayak[152], A. Nayaz[18], P.Y. Nechaeva[37], F. Nechansky[48], L. Nedic[127], T.J. Neep[20], A. Negri[73a,73b], M. Negrini[23b], C. Nellist[115], C. Nelson[105], K. Nelson[107], S. Nemecek[132], M. Nessi[36,h], M.S. Neubauer[163], F. Neuhaus[101], J. Neundorf[48], R. Newhouse[165], P.R. Newman[20], C.W. Ng[130], Y.W.Y. Ng[48], B. Ngair[117a], H.D.N. Nguyen[109], R.B. Nickerson[127], R. Nicolaidou[136], J. Nielsen[137], M. Niemeyer[55], J. Niermann[55], N. Nikiforou[36], V. Nikolaenko[37,a], I. Nikolic-Audit[128], K. Nikolopoulos[20], P. Nilsson[29], I. Ninca[48], H.R. Nindhito[56], G. Ninio[152], A. Nisati[75a], N. Nishu[2], R. Nisius[111], J-E. Nitschke[50], E.K. Nkadimeng[33g], T. Nobe[154], D.L. Noel[32], T. Nommensen[148], M.B. Norfolk[140], R.R.B. Norisam[97], B.J. Norman[34], M. Noury[35a], J. Novak[94], T. Novak[48], L. Novotny[133], R. Novotny[113], L. Nozka[123], K. Ntekas[160], N.M.J. Nunes De Moura Junior[83b], J. Ocariz[128], A. Ochi[85], I. Ochoa[131a], S. Oerdek[48,u], J.T. Offermann[39], A. Ogrodnik[134], A. Oh[102], C.C. Ohm[145], H. Oide[84], R. Oishi[154], M.L. Ojeda[48], Y. Okumura[154], L.F. Oleiro Seabra[131a], S.A. Olivares Pino[138d], D. Oliveira Damazio[29], D. Oliveira Goncalves[83a], J.L. Oliver[160], Ö.O. Öncel[54], A.P. O'Neill[19], A. Onofre[131a,131e], P.U.E. Onyisi[11], M.J. Oreglia[39], G.E. Orellana[91], D. Orestano[77a,77b], N. Orlando[13], R.S. Orr[156], V. O'Shea[59], L.M. Osojnak[129], R. Ospanov[62a], G. Otero y Garzon[30], H. Otono[89], P.S. Ott[63a], G.J. Ottino[17a], M. Ouchrif[35d], F. Ould-Saada[126], T. Ovsiannikova[139], M. Owen[59], R.E. Owen[135], K.Y. Oyulmaz[21a], V.E. Ozcan[21a], F. Ozturk[87], N. Ozturk[8], S. Ozturk[82], H.A. Pacey[127], A. Pacheco Pages[13], C. Padilla Aranda[13], G. Padovano[75a,75b], S. Pagan Griso[17a], G. Palacino[68], A. Palazzo[70a,70b], J. Pampel[24], J. Pan[173], T. Pan[64a], D.K. Panchal[11], C.E. Pandini[115], J.G. Panduro Vazquez[96], H.D. Pandya[1], H. Pang[14b], P. Pani[48], G. Panizzo[69a,69c], L. Panwar[128], L. Paolozzi[56], S. Parajuli[163], A. Paramonov[6], C. Paraskevopoulos[53], D. Paredes Hernandez[64b], A. Pareti[73a,73b], K.R. Park[41], T.H. Park[156], M.A. Parker[32], F. Parodi[57b,57a], E.W. Parrish[116], V.A. Parrish[52], J.A. Parsons[41], U. Parzefall[54], B. Pascual Dias[109], L. Pascual Dominguez[152], E. Pasqualucci[75a], S. Passaggio[57b], F. Pastore[96], P. Patel[87], U.M. Patel[51], J.R. Pater[102], T. Pauly[36], C.I. Pazos[159], J. Pearkes[144], M. Pedersen[126], R. Pedro[131a], S.V. Peleganchuk[37], O. Penc[36], E.A. Pender[52], G.D. Penn[173], K.E. Penski[110], M. Penzin[37], B.S. Peralva[83d], A.P. Pereira Peixoto[139], L. Pereira Sanchez[144], D.V. Perepelitsa[29,ah], E. Perez Codina[157a], M. Perganti[10], H. Pernegger[36], O. Perrin[40], K. Peters[48], R.F.Y. Peters[102], B.A. Petersen[36], T.C. Petersen[42], E. Petit[103], V. Petousis[133], C. Petridou[153,e], T. Petru[134], A. Petrukhin[142], M. Pettee[17a], N.E. Pettersson[36], A. Petukhov[37], K. Petukhova[134], R. Pezoa[138f], L. Pezzotti[36], G. Pezzullo[173], T.M. Pham[171], T. Pham[106], P.W. Phillips[135], G. Piacquadio[146], E. Pianori[17a], F. Piazza[124], R. Piegaia[30], D. Pietreanu[27b], A.D. Pilkington[102], M. Pinamonti[69a,69c], J.L. Pinfold[2], B.C. Pinheiro Pereira[131a], A.E. Pinto Pinoargote[101,136], L. Pintucci[69a,69c], K.M. Piper[147], A. Pirttikoski[56], D.A. Pizzi[34], L. Pizzimento[64b], A. Pizzini[115], M.-A. Pleier[29], V. Plesanovs[54], V. Pleskot[134], E. Plotnikova[38], G. Poddar[95], R. Poettgen[99], L. Poggioli[128], I. Pokharel[55], S. Polacek[134], G. Polesello[73a], A. Poley[143,157a], A. Polini[23b], C.S. Pollard[168], Z.B. Pollock[120], E. Pompa Pacchi[75a,75b], D. Ponomarenko[114], L. Pontecorvo[36], S. Popa[27a], G.A. Popeneciu[27d], A. Poreba[36], D.M. Portillo Quintero[157a], S. Pospisil[133], M.A. Postill[140], P. Postolache[27c],

JHEP11(2024)047

K. Potamianos[168], P.A. Potepa[86a], I.N. Potrap[38], C.J. Potter[32], H. Potti[1], J. Poveda[164], M.E. Pozo Astigarraga[36], A. Prades Ibanez[164], J. Pretel[54], D. Price[102], M. Primavera[70a], M.A. Principe Martin[100], R. Privara[123], T. Procter[59], M.L. Proffitt[139], N. Proklova[129], K. Prokofiev[64c], G. Proto[111], J. Proudfoot[6], M. Przybycien[86a], W.W. Przygoda[86b], A. Psallidas[46], J.E. Puddefoot[140], D. Pudzha[37], D. Pyatiizbyantseva[37], J. Qian[107], D. Qichen[102], Y. Qin[13], T. Qiu[52], A. Quadt[55], M. Queitsch-Maitland[102], G. Quetant[56], R.P. Quinn[165], G. Rabanal Bolanos[61], D. Rafanoharana[54], F. Ragusa[71a,71b], J.L. Rainbolt[39], J.A. Raine[56], S. Rajagopalan[29], E. Ramakoti[37], I.A. Ramirez-Berend[34], K. Ran[48,14e], N.P. Rapheeha[33g], H. Rasheed[27b], V. Raskina[128], D.F. Rassloff[63a], A. Rastogi[17a], S. Rave[101], B. Ravina[55], I. Ravinovich[170], M. Raymond[36], A.L. Read[126], N.P. Readioff[140], D.M. Rebuzzi[73a,73b], G. Redlinger[29], A.S. Reed[111], K. Reeves[26], J.A. Reidelsturz[172], D. Reikher[152], A. Rej[49], C. Rembser[36], M. Renda[27b], M.B. Rendel[111], F. Renner[48], A.G. Rennie[160], A.L. Rescia[48], S. Resconi[71a], M. Ressegotti[57b,57a], S. Rettie[36], J.G. Reyes Rivera[108], E. Reynolds[17a], O.L. Rezanova[37], P. Reznicek[134], H. Riani[35d], N. Ribaric[92], E. Ricci[78a,78b], R. Richter[111], S. Richter[47a,47b], E. Richter-Was[86b], M. Ridel[128], S. Ridouani[35d], P. Rieck[118], P. Riedler[36], E.M. Riefel[47a,47b], J.O. Rieger[115], M. Rijssenbeek[146], M. Rimoldi[36], L. Rinaldi[23b,23a], T.T. Rinn[29], M.P. Rinnagel[110], G. Ripellino[162], I. Riu[13], J.C. Rivera Vergara[166], F. Rizatdinova[122], E. Rizvi[95], B.R. Roberts[17a], S.H. Robertson[105,x], D. Robinson[32], C.M. Robles Gajardo[138f], M. Robles Manzano[101], A. Robson[59], A. Rocchi[76a,76b], C. Roda[74a,74b], S. Rodriguez Bosca[36], Y. Rodriguez Garcia[22a], A. Rodriguez Rodriguez[54], A.M. Rodríguez Vera[116], S. Roe[36], J.T. Roemer[160], A.R. Roepe-Gier[137], J. Roggel[172], O. Røhne[126], R.A. Rojas[104], C.P.A. Roland[128], J. Roloff[29], A. Romaniouk[37], E. Romano[73a,73b], M. Romano[23b], A.C. Romero Hernandez[163], N. Rompotis[93], L. Roos[128], S. Rosati[75a], B.J. Rosser[39], E. Rossi[127], E. Rossi[72a,72b], L.P. Rossi[61], L. Rossini[54], R. Rosten[120], M. Rotaru[27b], B. Rottler[54], C. Rougier[90], D. Rousseau[66], D. Rousso[32], A. Roy[163], S. Roy-Garand[156], A. Rozanov[103], Z.M.A. Rozario[59], Y. Rozen[151], A. Rubio Jimenez[164], A.J. Ruby[93], V.H. Ruelas Rivera[18], T.A. Ruggeri[1], A. Ruggiero[127], A. Ruiz-Martinez[164], A. Rummler[36], Z. Rurikova[54], N.A. Rusakovich[38], H.L. Russell[166], G. Russo[75a,75b], J.P. Rutherfoord[7], S. Rutherford Colmenares[32], K. Rybacki[92], M. Rybar[134], E.B. Rye[126], A. Ryzhov[44], J.A. Sabater Iglesias[56], P. Sabatini[164], H.F-W. Sadrozinski[137], F. Safai Tehrani[75a], B. Safarzadeh Samani[135], M. Safdari[144], S. Saha[1], M. Sahinsoy[111], A. Saibel[164], M. Saimpert[136], M. Saito[154], T. Saito[154], D. Salamani[36], A. Salnikov[144], J. Salt[164], A. Salvador Salas[152], D. Salvatore[43b,43a], F. Salvatore[147], A. Salzburger[36], D. Sammel[54], E. Sampson[92], D. Sampsonidis[153,e], D. Sampsonidou[124], J. Sánchez[164], V. Sanchez Sebastian[164], H. Sandaker[126], C.O. Sander[48], J.A. Sandesara[104], M. Sandhoff[172], C. Sandoval[22b], D.P.C. Sankey[135], T. Sano[88], A. Sansoni[53], L. Santi[75a,75b], C. Santoni[40], H. Santos[131a,131b], A. Santra[170], K.A. Saoucha[161], J.G. Saraiva[131a,131d], J. Sardain[7], O. Sasaki[84], K. Sato[158], C. Sauer[63b], F. Sauerburger[54], E. Sauvan[4], P. Savard[156,af], R. Sawada[154], C. Sawyer[135], L. Sawyer[98], I. Sayago Galvan[164], C. Sbarra[23b], A. Sbrizzi[23b,23a], T. Scanlon[97], J. Schaarschmidt[139], U. Schäfer[101], A.C. Schaffer[66,44], D. Schaile[110], R.D. Schamberger[146], C. Scharf[18], M.M. Schefer[19], V.A. Schegelsky[37], D. Scheirich[134], F. Schenck[18], M. Schernau[160],

C. Scheulen[55], C. Schiavi[57b,57a], M. Schioppa[43b,43a], B. Schlag[144,m], K.E. Schleicher[54], S. Schlenker[36], J. Schmeing[172], M.A. Schmidt[172], K. Schmieden[101], C. Schmitt[101], N. Schmitt[101], S. Schmitt[48], L. Schoeffel[136], A. Schoening[63b], P.G. Scholer[34], E. Schopf[127], M. Schott[101], J. Schovancova[36], S. Schramm[56], T. Schroer[56], H-C. Schultz-Coulon[63a], M. Schumacher[54], B.A. Schumm[137], Ph. Schune[136], A.J. Schuy[139], H.R. Schwartz[137], A. Schwartzman[144], T.A. Schwarz[107], Ph. Schwemling[136], R. Schwienhorst[108], A. Sciandra[137], G. Sciolla[26], F. Scuri[74a], C.D. Sebastiani[93], K. Sedlaczek[116], P. Seema[18], S.C. Seidel[113], A. Seiden[137], B.D. Seidlitz[41], C. Seitz[48], J.M. Seixas[83b], G. Sekhniaidze[72a], L. Selem[60], N. Semprini-Cesari[23b,23a], D. Sengupta[56], V. Senthilkumar[164], L. Serin[66], L. Serkin[69a,69b], M. Sessa[76a,76b], H. Severini[121], F. Sforza[57b,57a], A. Sfyrla[56], Q. Sha[14a], E. Shabalina[55], R. Shaheen[145], J.D. Shahinian[129], D. Shaked Renous[170], L.Y. Shan[14a], M. Shapiro[17a], A. Sharma[36], A.S. Sharma[165], P. Sharma[80], P.B. Shatalov[37], K. Shaw[147], S.M. Shaw[102], A. Shcherbakova[37], Q. Shen[62c,5], D.J. Sheppard[143], P. Sherwood[97], L. Shi[97], X. Shi[14a], C.O. Shimmin[173], J.D. Shinner[96], I.P.J. Shipsey[127], S. Shirabe[89], M. Shiyakova[38,v], J. Shlomi[170], M.J. Shochet[39], J. Shojaii[106], D.R. Shope[126], B. Shrestha[121], S. Shrestha[120,ai], E.M. Shrif[33g], M.J. Shroff[166], P. Sicho[132], A.M. Sickles[163], E. Sideras Haddad[33g], A. Sidoti[23b], F. Siegert[50], Dj. Sijacki[15], F. Sili[91], J.M. Silva[52], M.V. Silva Oliveira[29], S.B. Silverstein[47a], S. Simion[66], R. Simoniello[36], E.L. Simpson[59], H. Simpson[147], L.R. Simpson[107], N.D. Simpson[99], S. Simsek[82], S. Sindhu[55], P. Sinervo[156], S. Singh[156], S. Sinha[48], S. Sinha[102], M. Sioli[23b,23a], I. Siral[36], E. Sitnikova[48], J. Sjölin[47a,47b], A. Skaf[55], E. Skorda[20], P. Skubic[121], M. Slawinska[87], V. Smakhtin[170], B.H. Smart[135], S.Yu. Smirnov[37], Y. Smirnov[37], L.N. Smirnova[37,a], O. Smirnova[99], A.C. Smith[41], E.A. Smith[39], H.A. Smith[127], J.L. Smith[102], R. Smith[144], M. Smizanska[92], K. Smolek[133], A.A. Snesarev[37], S.R. Snider[156], H.L. Snoek[115], S. Snyder[29], R. Sobie[166,x], A. Soffer[152], C.A. Solans Sanchez[36], E.Yu. Soldatov[37], U. Soldevila[164], A.A. Solodkov[37], S. Solomon[26], A. Soloshenko[38], K. Solovieva[54], O.V. Solovyanov[40], V. Solovyev[37], P. Sommer[36], A. Sonay[13], W.Y. Song[157b], A. Sopczak[133], A.L. Sopio[97], F. Sopkova[28b], J.D. Sorenson[113], I.R. Sotarriva Alvarez[155], V. Sothilingam[63a], O.J. Soto Sandoval[138c,138b], S. Sottocornola[68], R. Soualah[161], Z. Soumaimi[35e], D. South[48], N. Soybelman[170], S. Spagnolo[70a,70b], M. Spalla[111], D. Sperlich[54], G. Spigo[36], S. Spinali[92], D.P. Spiteri[59], M. Spousta[134], E.J. Staats[34], R. Stamen[63a], A. Stampekis[20], M. Standke[24], E. Stanecka[87], M.V. Stange[50], B. Stanislaus[17a], M.M. Stanitzki[48], B. Stapf[48], E.A. Starchenko[37], G.H. Stark[137], J. Stark[90], P. Staroba[132], P. Starovoitov[63a], S. Stärz[105], R. Staszewski[87], G. Stavropoulos[46], J. Steentoft[162], P. Steinberg[29], B. Stelzer[143,157a], H.J. Stelzer[130], O. Stelzer-Chilton[157a], H. Stenzel[58], T.J. Stevenson[147], G.A. Stewart[36], J.R. Stewart[122], M.C. Stockton[36], G. Stoicea[27b], M. Stolarski[131a], S. Stonjek[111], A. Straessner[50], J. Strandberg[145], S. Strandberg[47a,47b], M. Stratmann[172], M. Strauss[121], T. Strebler[103], P. Strizenec[28b], R. Ströhmer[167], D.M. Strom[124], R. Stroynowski[44], A. Strubig[47a,47b], S.A. Stucci[29], B. Stugu[16], J. Stupak[121], N.A. Styles[48], D. Su[144], S. Su[62a], W. Su[62d], X. Su[62a], D. Suchy[28a], K. Sugizaki[154], V.V. Sulin[37], M.J. Sullivan[93], D.M.S. Sultan[127], L. Sultanaliyeva[37], S. Sultansoy[3b], T. Sumida[88], S. Sun[107], S. Sun[171], O. Sunneborn Gudnadottir[162],

JHEP11(2024)047

N. Sur[103], M.R. Sutton[147], H. Suzuki[158], M. Svatos[132], M. Swiatlowski[157a], T. Swirski[167], I. Sykora[28a], M. Sykora[134], T. Sykora[134], D. Ta[101], K. Tackmann[48,u], A. Taffard[160], R. Tafirout[157a], J.S. Tafoya Vargas[66], Y. Takubo[84], M. Talby[103], A.A. Talyshev[37], K.C. Tam[64b], N.M. Tamir[152], A. Tanaka[154], J. Tanaka[154], R. Tanaka[66], M. Tanasini[57b,57a], Z. Tao[165], S. Tapia Araya[138f], S. Tapprogge[101], A. Tarek Abouelfadl Mohamed[108], S. Tarem[151], K. Tariq[14a], G. Tarna[103,27b], G.F. Tartarelli[71a], P. Tas[134], M. Tasevsky[132], E. Tassi[43b,43a], A.C. Tate[163], G. Tateno[154], Y. Tayalati[35e,w], G.N. Taylor[106], W. Taylor[157b], A.S. Tee[171], R. Teixeira De Lima[144], P. Teixeira-Dias[96], J.J. Teoh[156], K. Terashi[154], J. Terron[100], S. Terzo[13], M. Testa[53], R.J. Teuscher[156,x], A. Thaler[79], O. Theiner[56], N. Themistokleous[52], T. Theveneaux-Pelzer[103], O. Thielmann[172], D.W. Thomas[96], J.P. Thomas[20], E.A. Thompson[17a], P.D. Thompson[20], E. Thomson[129], R.E. Thornberry[44], Y. Tian[55], V. Tikhomirov[37,a], Yu.A. Tikhonov[37], S. Timoshenko[37], D. Timoshyn[134], E.X.L. Ting[1], P. Tipton[173], S.H. Tlou[33g], K. Todome[155], S. Todorova-Nova[134], S. Todt[50], M. Togawa[84], J. Tojo[89], S. Tokár[28a], K. Tokushuku[84], O. Toldaiev[68], R. Tombs[32], M. Tomoto[84,112], L. Tompkins[144,m], K.W. Topolnicki[86b], E. Torrence[124], H. Torres[90], E. Torró Pastor[164], M. Toscani[30], C. Tosciri[39], M. Tost[11], D.R. Tovey[140], A. Traeet[16], I.S. Trandafir[27b], T. Trefzger[167], A. Tricoli[29], I.M. Trigger[157a], S. Trincaz-Duvoid[128], D.A. Trischuk[26], B. Trocmé[60], L. Truong[33c], M. Trzebinski[87], A. Trzupek[87], F. Tsai[146], M. Tsai[107], A. Tsiamis[153,e], P.V. Tsiareshka[37], S. Tsigaridas[157a], A. Tsirigotis[153,s], V. Tsiskaridze[156], E.G. Tskhadadze[150a], M. Tsopoulou[153], Y. Tsujikawa[88], I.I. Tsukerman[37], V. Tsulaia[17a], S. Tsuno[84], K. Tsuri[119], D. Tsybychev[146], Y. Tu[64b], A. Tudorache[27b], V. Tudorache[27b], A.N. Tuna[61], S. Turchikhin[57b,57a], I. Turk Cakir[3a], R. Turra[71a], T. Turtuvshin[38,y], P.M. Tuts[41], S. Tzamarias[153,e], E. Tzovara[101], F. Ukegawa[158], P.A. Ulloa Poblete[138c,138b], E.N. Umaka[29], G. Unal[36], A. Undrus[29], G. Unel[160], J. Urban[28b], P. Urquijo[106], P. Urrejola[138a], G. Usai[8], R. Ushioda[155], M. Usman[109], Z. Uysal[82], V. Vacek[133], B. Vachon[105], K.O.H. Vadla[126], T. Vafeiadis[36], A. Vaitkus[97], C. Valderanis[110], E. Valdes Santurio[47a,47b], M. Valente[157a], S. Valentinetti[23b,23a], A. Valero[164], E. Valiente Moreno[164], A. Vallier[90], J.A. Valls Ferrer[164], D.R. Van Arneman[115], T.R. Van Daalen[139], A. Van Der Graaf[49], P. Van Gemmeren[6], M. Van Rijnbach[126], S. Van Stroud[97], I. Van Vulpen[115], P. Vana[134], M. Vanadia[76a,76b], W. Vandelli[36], E.R. Vandewall[122], D. Vannicola[152], L. Vannoli[53], R. Vari[75a], E.W. Varnes[7], C. Varni[17b], T. Varol[149], D. Varouchas[66], L. Varriale[164], K.E. Varvell[148], M.E. Vasile[27b], L. Vaslin[84], G.A. Vasquez[166], A. Vasyukov[38], R. Vavricka[101], F. Vazeille[40], T. Vazquez Schroeder[36], J. Veatch[31], V. Vecchio[102], M.J. Veen[104], I. Veliscek[29], L.M. Veloce[156], F. Veloso[131a,131c], S. Veneziano[75a], A. Ventura[70a,70b], S. Ventura Gonzalez[136], A. Verbytskyi[111], M. Verducci[74a,74b], C. Vergis[24], M. Verissimo De Araujo[83b], W. Verkerke[115], J.C. Vermeulen[115], C. Vernieri[144], M. Vessella[104], M.C. Vetterli[143,af], A. Vgenopoulos[153,e], N. Viaux Maira[138f], T. Vickey[140], O.E. Vickey Boeriu[140], G.H.A. Viehhauser[127], L. Vigani[63b], M. Villa[23b,23a], M. Villaplana Perez[164], E.M. Villhauer[52], E. Vilucchi[53], M.G. Vincter[34], G.S. Virdee[20], A. Vishwakarma[52], A. Visibile[115], C. Vittori[36], I. Vivarelli[23b,23a], E. Voevodina[111], F. Vogel[110], J.C. Voigt[50], P. Vokac[133], Yu. Volkotrub[86b], J. Von Ahnen[48],

E. Von Toerne[24], B. Vormwald[36], V. Vorobel[134], K. Vorobev[37], M. Vos[164], K. Voss[142], M. Vozak[115], L. Vozdecky[121], N. Vranjes[15], M. Vranjes Milosavljevic[15], M. Vreeswijk[115], N.K. Vu[62d,62c], R. Vuillermet[36], O. Vujinovic[101], I. Vukotic[39], S. Wada[158], C. Wagner[104], J.M. Wagner[17a], W. Wagner[172], S. Wahdan[172], H. Wahlberg[91], M. Wakida[112], J. Walder[135], R. Walker[110], W. Walkowiak[142], A. Wall[129], E.J. Wallin[99], T. Wamorkar[6], A.Z. Wang[137], C. Wang[101], C. Wang[11], H. Wang[17a], J. Wang[64c], R.-J. Wang[101], R. Wang[61], R. Wang[6], S.M. Wang[149], S. Wang[62b], T. Wang[62a], W.T. Wang[80], W. Wang[14a], X. Wang[14c], X. Wang[163], X. Wang[62c], Y. Wang[62d], Y. Wang[14c], Z. Wang[107], Z. Wang[62d,51,62c], Z. Wang[107], A. Warburton[105], R.J. Ward[20], N. Warrack[59], S. Waterhouse[96], A.T. Watson[20], H. Watson[59], M.F. Watson[20], E. Watton[59,135], G. Watts[139], B.M. Waugh[97], C. Weber[29], H.A. Weber[18], M.S. Weber[19], S.M. Weber[63a], C. Wei[62a], Y. Wei[127], A.R. Weidberg[127], E.J. Weik[118], J. Weingarten[49], M. Weirich[101], C. Weiser[54], C.J. Wells[48], T. Wenaus[29], B. Wendland[49], T. Wengler[36], N.S. Wenke[111], N. Wermes[24], M. Wessels[63a], A.M. Wharton[92], A.S. White[61], A. White[8], M.J. White[1], D. Whiteson[160], L. Wickremasinghe[125], W. Wiedenmann[171], M. Wielers[135], C. Wiglesworth[42], D.J. Wilbern[121], H.G. Wilkens[36], D.M. Williams[41], H.H. Williams[129], S. Williams[32], S. Willocq[104], B.J. Wilson[102], P.J. Windischhofer[39], F.I. Winkel[30], F. Winklmeier[124], B.T. Winter[54], J.K. Winter[102], M. Wittgen[144], M. Wobisch[98], Z. Wolffs[115], J. Wollrath[160], M.W. Wolter[87], H. Wolters[131a,131c], M.C. Wong[137], E.L. Woodward[41], S.D. Worm[48], B.K. Wosiek[87], K.W. Woźniak[87], S. Wozniewski[55], K. Wraight[59], C. Wu[20], M. Wu[14d], M. Wu[114], S.L. Wu[171], X. Wu[56], Y. Wu[62a], Z. Wu[4], J. Wuerzinger[111,ad], T.R. Wyatt[102], B.M. Wynne[52], S. Xella[42], L. Xia[14c], M. Xia[14b], J. Xiang[64c], M. Xie[62a], X. Xie[62a], S. Xin[14a,14e], A. Xiong[124], J. Xiong[17a], D. Xu[14a], H. Xu[62a], L. Xu[62a], R. Xu[129], T. Xu[107], Y. Xu[14b], Z. Xu[52], Z. Xu[14c], B. Yabsley[148], S. Yacoob[33a], Y. Yamaguchi[155], E. Yamashita[154], H. Yamauchi[158], T. Yamazaki[17a], Y. Yamazaki[85], J. Yan[62c], S. Yan[59], Z. Yan[104], H.J. Yang[62c,62d], H.T. Yang[62a], S. Yang[62a], T. Yang[64c], X. Yang[36], X. Yang[14a], Y. Yang[44], Y. Yang[62a], Z. Yang[62a], W-M. Yao[17a], H. Ye[14c], H. Ye[55], J. Ye[14a], S. Ye[29], X. Ye[62a], Y. Yeh[97], I. Yeletskikh[38], B. Yeo[17b], M.R. Yexley[97], P. Yin[41], K. Yorita[169], S. Younas[27b], C.J.S. Young[36], C. Young[144], C. Yu[14a,14e], Y. Yu[62a], M. Yuan[107], R. Yuan[62b], L. Yue[97], M. Zaazoua[62a], B. Zabinski[87], E. Zaid[52], Z.K. Zak[87], T. Zakareishvili[164], N. Zakharchuk[34], S. Zambito[56], J.A. Zamora Saa[138d,138b], J. Zang[154], D. Zanzi[54], O. Zaplatilek[133], C. Zeitnitz[172], H. Zeng[14a], J.C. Zeng[163], D.T. Zenger Jr[26], O. Zenin[37], T. Ženiš[28a], S. Zenz[95], S. Zerradi[35a], D. Zerwas[66], M. Zhai[14a,14e], D.F. Zhang[140], J. Zhang[62b], J. Zhang[6], K. Zhang[14a,14e], L. Zhang[14c], P. Zhang[14a,14e], R. Zhang[171], S. Zhang[107], S. Zhang[44], T. Zhang[154], X. Zhang[62c], X. Zhang[62b], Y. Zhang[62c,5], Y. Zhang[97], Y. Zhang[14c], Z. Zhang[17a], Z. Zhang[66], H. Zhao[139], T. Zhao[62b], Y. Zhao[137], Z. Zhao[62a], A. Zhemchugov[38], J. Zheng[14c], K. Zheng[163], X. Zheng[62a], Z. Zheng[144], D. Zhong[163], B. Zhou[107], H. Zhou[7], N. Zhou[62c], Y. Zhou[14c], Y. Zhou[7], C.G. Zhu[62b], J. Zhu[107], Y. Zhu[62c], Y. Zhu[62a], X. Zhuang[14a], K. Zhukov[37], N.I. Zimine[38], J. Zinsser[63b], M. Ziolkowski[142], L. Živković[15], A. Zoccoli[23b,23a], K. Zoch[61], T.G. Zorbas[140], O. Zormpa[46], W. Zou[41], L. Zwalinski[36]

[1] *Department of Physics, University of Adelaide, Adelaide; Australia*

JHEP11(2024)047

[2] *Department of Physics, University of Alberta, Edmonton AB; Canada*
[3] [(a)] *Department of Physics, Ankara University, Ankara;*[(b)] *Division of Physics, TOBB University of Economics and Technology, Ankara; Türkiye*
[4] *LAPP, Université Savoie Mont Blanc, CNRS/IN2P3, Annecy; France*
[5] *APC, Université Paris Cité, CNRS/IN2P3, Paris; France*
[6] *High Energy Physics Division, Argonne National Laboratory, Argonne IL; United States of America*
[7] *Department of Physics, University of Arizona, Tucson AZ; United States of America*
[8] *Department of Physics, University of Texas at Arlington, Arlington TX; United States of America*
[9] *Physics Department, National and Kapodistrian University of Athens, Athens; Greece*
[10] *Physics Department, National Technical University of Athens, Zografou; Greece*
[11] *Department of Physics, University of Texas at Austin, Austin TX; United States of America*
[12] *Institute of Physics, Azerbaijan Academy of Sciences, Baku; Azerbaijan*
[13] *Institut de Física d'Altes Energies (IFAE), Barcelona Institute of Science and Technology, Barcelona; Spain*
[14] [(a)] *Institute of High Energy Physics, Chinese Academy of Sciences, Beijing;*[(b)] *Physics Department, Tsinghua University, Beijing;*[(c)] *Department of Physics, Nanjing University, Nanjing;*[(d)] *School of Science, Shenzhen Campus of Sun Yat-sen University;*[(e)] *University of Chinese Academy of Science (UCAS), Beijing; China*
[15] *Institute of Physics, University of Belgrade, Belgrade; Serbia*
[16] *Department for Physics and Technology, University of Bergen, Bergen; Norway*
[17] [(a)] *Physics Division, Lawrence Berkeley National Laboratory, Berkeley CA;*[(b)] *University of California, Berkeley CA; United States of America*
[18] *Institut für Physik, Humboldt Universität zu Berlin, Berlin; Germany*
[19] *Albert Einstein Center for Fundamental Physics and Laboratory for High Energy Physics, University of Bern, Bern; Switzerland*
[20] *School of Physics and Astronomy, University of Birmingham, Birmingham; United Kingdom*
[21] [(a)] *Department of Physics, Bogazici University, Istanbul;*[(b)] *Department of Physics Engineering, Gaziantep University, Gaziantep;*[(c)] *Department of Physics, Istanbul University, Istanbul; Türkiye*
[22] [(a)] *Facultad de Ciencias y Centro de Investigaciónes, Universidad Antonio Nariño, Bogotá;*[(b)] *Departamento de Física, Universidad Nacional de Colombia, Bogotá; Colombia*
[23] [(a)] *Dipartimento di Fisica e Astronomia A. Righi, Università di Bologna, Bologna;*[(b)] *INFN Sezione di Bologna; Italy*
[24] *Physikalisches Institut, Universität Bonn, Bonn; Germany*
[25] *Department of Physics, Boston University, Boston MA; United States of America*
[26] *Department of Physics, Brandeis University, Waltham MA; United States of America*
[27] [(a)] *Transilvania University of Brasov, Brasov;*[(b)] *Horia Hulubei National Institute of Physics and Nuclear Engineering, Bucharest;*[(c)] *Department of Physics, Alexandru Ioan Cuza University of Iasi, Iasi;*[(d)] *National Institute for Research and Development of Isotopic and Molecular Technologies, Physics Department, Cluj-Napoca;*[(e)] *National University of Science and Technology Politechnica, Bucharest;*[(f)] *West University in Timisoara, Timisoara;*[(g)] *Faculty of Physics, University of Bucharest, Bucharest; Romania*
[28] [(a)] *Faculty of Mathematics, Physics and Informatics, Comenius University, Bratislava;*[(b)] *Department of Subnuclear Physics, Institute of Experimental Physics of the Slovak Academy of Sciences, Kosice; Slovak Republic*
[29] *Physics Department, Brookhaven National Laboratory, Upton NY; United States of America*
[30] *Universidad de Buenos Aires, Facultad de Ciencias Exactas y Naturales, Departamento de Física, y CONICET, Instituto de Física de Buenos Aires (IFIBA), Buenos Aires; Argentina*
[31] *California State University, CA; United States of America*
[32] *Cavendish Laboratory, University of Cambridge, Cambridge; United Kingdom*
[33] [(a)] *Department of Physics, University of Cape Town, Cape Town;*[(b)] *iThemba Labs, Western Cape;*[(c)] *Department of Mechanical Engineering Science, University of Johannesburg, Johannesburg;*[(d)] *National Institute of Physics, University of the Philippines Diliman (Philippines);*[(e)] *University of South Africa, Department of Physics, Pretoria;*[(f)] *University of Zululand, KwaDlangezwa;*[(g)] *School of Physics, University of the Witwatersrand, Johannesburg; South Africa*

JHEP11(2024)047

[34] *Department of Physics, Carleton University, Ottawa ON; Canada*
[35] [(a)] *Faculté des Sciences Ain Chock, Université Hassan II de Casablanca;* [(b)] *Faculté des Sciences, Université Ibn-Tofail, Kénitra;* [(c)] *Faculté des Sciences Semlalia, Université Cadi Ayyad, LPHEA-Marrakech;* [(d)] *LPMR, Faculté des Sciences, Université Mohamed Premier, Oujda;* [(e)] *Faculté des sciences, Université Mohammed V, Rabat;* [(f)] *Institute of Applied Physics, Mohammed VI Polytechnic University, Ben Guerir; Morocco*
[36] *CERN, Geneva; Switzerland*
[37] *Affiliated with an institute covered by a cooperation agreement with CERN*
[38] *Affiliated with an international laboratory covered by a cooperation agreement with CERN*
[39] *Enrico Fermi Institute, University of Chicago, Chicago IL; United States of America*
[40] *LPC, Université Clermont Auvergne, CNRS/IN2P3, Clermont-Ferrand; France*
[41] *Nevis Laboratory, Columbia University, Irvington NY; United States of America*
[42] *Niels Bohr Institute, University of Copenhagen, Copenhagen; Denmark*
[43] [(a)] *Dipartimento di Fisica, Università della Calabria, Rende;* [(b)] *INFN Gruppo Collegato di Cosenza, Laboratori Nazionali di Frascati; Italy*
[44] *Physics Department, Southern Methodist University, Dallas TX; United States of America*
[45] *Physics Department, University of Texas at Dallas, Richardson TX; United States of America*
[46] *National Centre for Scientific Research "Demokritos", Agia Paraskevi; Greece*
[47] [(a)] *Department of Physics, Stockholm University;* [(b)] *Oskar Klein Centre, Stockholm; Sweden*
[48] *Deutsches Elektronen-Synchrotron DESY, Hamburg and Zeuthen; Germany*
[49] *Fakultät Physik , Technische Universität Dortmund, Dortmund; Germany*
[50] *Institut für Kern- und Teilchenphysik, Technische Universität Dresden, Dresden; Germany*
[51] *Department of Physics, Duke University, Durham NC; United States of America*
[52] *SUPA - School of Physics and Astronomy, University of Edinburgh, Edinburgh; United Kingdom*
[53] *INFN e Laboratori Nazionali di Frascati, Frascati; Italy*
[54] *Physikalisches Institut, Albert-Ludwigs-Universität Freiburg, Freiburg; Germany*
[55] *II. Physikalisches Institut, Georg-August-Universität Göttingen, Göttingen; Germany*
[56] *Département de Physique Nucléaire et Corpusculaire, Université de Genève, Genève; Switzerland*
[57] [(a)] *Dipartimento di Fisica, Università di Genova, Genova;* [(b)] *INFN Sezione di Genova; Italy*
[58] *II. Physikalisches Institut, Justus-Liebig-Universität Giessen, Giessen; Germany*
[59] *SUPA - School of Physics and Astronomy, University of Glasgow, Glasgow; United Kingdom*
[60] *LPSC, Université Grenoble Alpes, CNRS/IN2P3, Grenoble INP, Grenoble; France*
[61] *Laboratory for Particle Physics and Cosmology, Harvard University, Cambridge MA; United States of America*
[62] [(a)] *Department of Modern Physics and State Key Laboratory of Particle Detection and Electronics, University of Science and Technology of China, Hefei;* [(b)] *Institute of Frontier and Interdisciplinary Science and Key Laboratory of Particle Physics and Particle Irradiation (MOE), Shandong University, Qingdao;* [(c)] *School of Physics and Astronomy, Shanghai Jiao Tong University, Key Laboratory for Particle Astrophysics and Cosmology (MOE), SKLPPC, Shanghai;* [(d)] *Tsung-Dao Lee Institute, Shanghai;* [(e)] *School of Physics and Microelectronics, Zhengzhou University; China*
[63] [(a)] *Kirchhoff-Institut für Physik, Ruprecht-Karls-Universität Heidelberg, Heidelberg;* [(b)] *Physikalisches Institut, Ruprecht-Karls-Universität Heidelberg, Heidelberg; Germany*
[64] [(a)] *Department of Physics, Chinese University of Hong Kong, Shatin, N.T., Hong Kong;* [(b)] *Department of Physics, University of Hong Kong, Hong Kong;* [(c)] *Department of Physics and Institute for Advanced Study, Hong Kong University of Science and Technology, Clear Water Bay, Kowloon, Hong Kong; China*
[65] *Department of Physics, National Tsing Hua University, Hsinchu; Taiwan*
[66] *IJCLab, Université Paris-Saclay, CNRS/IN2P3, 91405, Orsay; France*
[67] *Centro Nacional de Microelectrónica (IMB-CNM-CSIC), Barcelona; Spain*
[68] *Department of Physics, Indiana University, Bloomington IN; United States of America*
[69] [(a)] *INFN Gruppo Collegato di Udine, Sezione di Trieste, Udine;* [(b)] *ICTP, Trieste;* [(c)] *Dipartimento Politecnico di Ingegneria e Architettura, Università di Udine, Udine; Italy*
[70] [(a)] *INFN Sezione di Lecce;* [(b)] *Dipartimento di Matematica e Fisica, Università del Salento, Lecce; Italy*
[71] [(a)] *INFN Sezione di Milano;* [(b)] *Dipartimento di Fisica, Università di Milano, Milano; Italy*
[72] [(a)] *INFN Sezione di Napoli;* [(b)] *Dipartimento di Fisica, Università di Napoli, Napoli; Italy*

JHEP11(2024)047

[73] [(a)] *INFN Sezione di Pavia;* [(b)] *Dipartimento di Fisica, Università di Pavia, Pavia; Italy*
[74] [(a)] *INFN Sezione di Pisa;* [(b)] *Dipartimento di Fisica E. Fermi, Università di Pisa, Pisa; Italy*
[75] [(a)] *INFN Sezione di Roma;* [(b)] *Dipartimento di Fisica, Sapienza Università di Roma, Roma; Italy*
[76] [(a)] *INFN Sezione di Roma Tor Vergata;* [(b)] *Dipartimento di Fisica, Università di Roma Tor Vergata, Roma; Italy*
[77] [(a)] *INFN Sezione di Roma Tre;* [(b)] *Dipartimento di Matematica e Fisica, Università Roma Tre, Roma; Italy*
[78] [(a)] *INFN-TIFPA;* [(b)] *Università degli Studi di Trento, Trento; Italy*
[79] *Universität Innsbruck, Department of Astro and Particle Physics, Innsbruck; Austria*
[80] *University of Iowa, Iowa City IA; United States of America*
[81] *Department of Physics and Astronomy, Iowa State University, Ames IA; United States of America*
[82] *Istinye University, Sariyer, Istanbul; Türkiye*
[83] [(a)] *Departamento de Engenharia Elétrica, Universidade Federal de Juiz de Fora (UFJF), Juiz de Fora;* [(b)] *Universidade Federal do Rio De Janeiro COPPE/EE/IF, Rio de Janeiro;* [(c)] *Instituto de Física, Universidade de São Paulo, São Paulo;* [(d)] *Rio de Janeiro State University, Rio de Janeiro;* [(e)] *Federal University of Bahia, Bahia; Brazil*
[84] *KEK, High Energy Accelerator Research Organization, Tsukuba; Japan*
[85] *Graduate School of Science, Kobe University, Kobe; Japan*
[86] [(a)] *AGH University of Krakow, Faculty of Physics and Applied Computer Science, Krakow;* [(b)] *Marian Smoluchowski Institute of Physics, Jagiellonian University, Krakow; Poland*
[87] *Institute of Nuclear Physics Polish Academy of Sciences, Krakow; Poland*
[88] *Faculty of Science, Kyoto University, Kyoto; Japan*
[89] *Research Center for Advanced Particle Physics and Department of Physics, Kyushu University, Fukuoka; Japan*
[90] *L2IT, Université de Toulouse, CNRS/IN2P3, UPS, Toulouse; France*
[91] *Instituto de Física La Plata, Universidad Nacional de La Plata and CONICET, La Plata; Argentina*
[92] *Physics Department, Lancaster University, Lancaster; United Kingdom*
[93] *Oliver Lodge Laboratory, University of Liverpool, Liverpool; United Kingdom*
[94] *Department of Experimental Particle Physics, Jožef Stefan Institute and Department of Physics, University of Ljubljana, Ljubljana; Slovenia*
[95] *School of Physics and Astronomy, Queen Mary University of London, London; United Kingdom*
[96] *Department of Physics, Royal Holloway University of London, Egham; United Kingdom*
[97] *Department of Physics and Astronomy, University College London, London; United Kingdom*
[98] *Louisiana Tech University, Ruston LA; United States of America*
[99] *Fysiska institutionen, Lunds universitet, Lund; Sweden*
[100] *Departamento de Física Teorica C-15 and CIAFF, Universidad Autónoma de Madrid, Madrid; Spain*
[101] *Institut für Physik, Universität Mainz, Mainz; Germany*
[102] *School of Physics and Astronomy, University of Manchester, Manchester; United Kingdom*
[103] *CPPM, Aix-Marseille Université, CNRS/IN2P3, Marseille; France*
[104] *Department of Physics, University of Massachusetts, Amherst MA; United States of America*
[105] *Department of Physics, McGill University, Montreal QC; Canada*
[106] *School of Physics, University of Melbourne, Victoria; Australia*
[107] *Department of Physics, University of Michigan, Ann Arbor MI; United States of America*
[108] *Department of Physics and Astronomy, Michigan State University, East Lansing MI; United States of America*
[109] *Group of Particle Physics, University of Montreal, Montreal QC; Canada*
[110] *Fakultät für Physik, Ludwig-Maximilians-Universität München, München; Germany*
[111] *Max-Planck-Institut für Physik (Werner-Heisenberg-Institut), München; Germany*
[112] *Graduate School of Science and Kobayashi-Maskawa Institute, Nagoya University, Nagoya; Japan*
[113] *Department of Physics and Astronomy, University of New Mexico, Albuquerque NM; United States of America*
[114] *Institute for Mathematics, Astrophysics and Particle Physics, Radboud University/Nikhef, Nijmegen; Netherlands*
[115] *Nikhef National Institute for Subatomic Physics and University of Amsterdam, Amsterdam; Netherlands*

JHEP11(2024)047

[116] *Department of Physics, Northern Illinois University, DeKalb IL; United States of America*
[117] [(a)] *New York University Abu Dhabi, Abu Dhabi;*[(b)] *United Arab Emirates University, Al Ain; United Arab Emirates*
[118] *Department of Physics, New York University, New York NY; United States of America*
[119] *Ochanomizu University, Otsuka, Bunkyo-ku, Tokyo; Japan*
[120] *Ohio State University, Columbus OH; United States of America*
[121] *Homer L. Dodge Department of Physics and Astronomy, University of Oklahoma, Norman OK; United States of America*
[122] *Department of Physics, Oklahoma State University, Stillwater OK; United States of America*
[123] *Palacký University, Joint Laboratory of Optics, Olomouc; Czech Republic*
[124] *Institute for Fundamental Science, University of Oregon, Eugene, OR; United States of America*
[125] *Graduate School of Science, Osaka University, Osaka; Japan*
[126] *Department of Physics, University of Oslo, Oslo; Norway*
[127] *Department of Physics, Oxford University, Oxford; United Kingdom*
[128] *LPNHE, Sorbonne Université, Université Paris Cité, CNRS/IN2P3, Paris; France*
[129] *Department of Physics, University of Pennsylvania, Philadelphia PA; United States of America*
[130] *Department of Physics and Astronomy, University of Pittsburgh, Pittsburgh PA; United States of America*
[131] [(a)] *Laboratório de Instrumentação e Física Experimental de Partículas - LIP, Lisboa;*[(b)] *Departamento de Física, Faculdade de Ciências, Universidade de Lisboa, Lisboa;*[(c)] *Departamento de Física, Universidade de Coimbra, Coimbra;*[(d)] *Centro de Física Nuclear da Universidade de Lisboa, Lisboa;*[(e)] *Departamento de Física, Universidade do Minho, Braga;*[(f)] *Departamento de Física Teórica y del Cosmos, Universidad de Granada, Granada (Spain);*[(g)] *Departamento de Física, Instituto Superior Técnico, Universidade de Lisboa, Lisboa; Portugal*
[132] *Institute of Physics of the Czech Academy of Sciences, Prague; Czech Republic*
[133] *Czech Technical University in Prague, Prague; Czech Republic*
[134] *Charles University, Faculty of Mathematics and Physics, Prague; Czech Republic*
[135] *Particle Physics Department, Rutherford Appleton Laboratory, Didcot; United Kingdom*
[136] *IRFU, CEA, Université Paris-Saclay, Gif-sur-Yvette; France*
[137] *Santa Cruz Institute for Particle Physics, University of California Santa Cruz, Santa Cruz CA; United States of America*
[138] [(a)] *Departamento de Física, Pontificia Universidad Católica de Chile, Santiago;*[(b)] *Millennium Institute for Subatomic physics at high energy frontier (SAPHIR), Santiago;*[(c)] *Instituto de Investigación Multidisciplinario en Ciencia y Tecnología, y Departamento de Física, Universidad de La Serena;*[(d)] *Universidad Andres Bello, Department of Physics, Santiago;*[(e)] *Instituto de Alta Investigación, Universidad de Tarapacá, Arica;*[(f)] *Departamento de Física, Universidad Técnica Federico Santa María, Valparaíso; Chile*
[139] *Department of Physics, University of Washington, Seattle WA; United States of America*
[140] *Department of Physics and Astronomy, University of Sheffield, Sheffield; United Kingdom*
[141] *Department of Physics, Shinshu University, Nagano; Japan*
[142] *Department Physik, Universität Siegen, Siegen; Germany*
[143] *Department of Physics, Simon Fraser University, Burnaby BC; Canada*
[144] *SLAC National Accelerator Laboratory, Stanford CA; United States of America*
[145] *Department of Physics, Royal Institute of Technology, Stockholm; Sweden*
[146] *Departments of Physics and Astronomy, Stony Brook University, Stony Brook NY; United States of America*
[147] *Department of Physics and Astronomy, University of Sussex, Brighton; United Kingdom*
[148] *School of Physics, University of Sydney, Sydney; Australia*
[149] *Institute of Physics, Academia Sinica, Taipei; Taiwan*
[150] [(a)] *E. Andronikashvili Institute of Physics, Iv. Javakhishvili Tbilisi State University, Tbilisi;*[(b)] *High Energy Physics Institute, Tbilisi State University, Tbilisi;*[(c)] *University of Georgia, Tbilisi; Georgia*
[151] *Department of Physics, Technion, Israel Institute of Technology, Haifa; Israel*
[152] *Raymond and Beverly Sackler School of Physics and Astronomy, Tel Aviv University, Tel Aviv; Israel*
[153] *Department of Physics, Aristotle University of Thessaloniki, Thessaloniki; Greece*

JHEP11(2024)047

[154] International Center for Elementary Particle Physics and Department of Physics, University of Tokyo, Tokyo; Japan
[155] Department of Physics, Tokyo Institute of Technology, Tokyo; Japan
[156] Department of Physics, University of Toronto, Toronto ON; Canada
[157] [(a)] TRIUMF, Vancouver BC;[(b)] Department of Physics and Astronomy, York University, Toronto ON; Canada
[158] Division of Physics and Tomonaga Center for the History of the Universe, Faculty of Pure and Applied Sciences, University of Tsukuba, Tsukuba; Japan
[159] Department of Physics and Astronomy, Tufts University, Medford MA; United States of America
[160] Department of Physics and Astronomy, University of California Irvine, Irvine CA; United States of America
[161] University of Sharjah, Sharjah; United Arab Emirates
[162] Department of Physics and Astronomy, University of Uppsala, Uppsala; Sweden
[163] Department of Physics, University of Illinois, Urbana IL; United States of America
[164] Instituto de Física Corpuscular (IFIC), Centro Mixto Universidad de Valencia - CSIC, Valencia; Spain
[165] Department of Physics, University of British Columbia, Vancouver BC; Canada
[166] Department of Physics and Astronomy, University of Victoria, Victoria BC; Canada
[167] Fakultät für Physik und Astronomie, Julius-Maximilians-Universität Würzburg, Würzburg; Germany
[168] Department of Physics, University of Warwick, Coventry; United Kingdom
[169] Waseda University, Tokyo; Japan
[170] Department of Particle Physics and Astrophysics, Weizmann Institute of Science, Rehovot; Israel
[171] Department of Physics, University of Wisconsin, Madison WI; United States of America
[172] Fakultät für Mathematik und Naturwissenschaften, Fachgruppe Physik, Bergische Universität Wuppertal, Wuppertal; Germany
[173] Department of Physics, Yale University, New Haven CT; United States of America

[a] Also Affiliated with an institute covered by a cooperation agreement with CERN
[b] Also at An-Najah National University, Nablus; Palestine
[c] Also at Borough of Manhattan Community College, City University of New York, New York NY; United States of America
[d] Also at Center for High Energy Physics, Peking University; China
[e] Also at Center for Interdisciplinary Research and Innovation (CIRI-AUTH), Thessaloniki; Greece
[f] Also at Centro Studi e Ricerche Enrico Fermi; Italy
[g] Also at CERN, Geneva; Switzerland
[h] Also at Département de Physique Nucléaire et Corpusculaire, Université de Genève, Genève; Switzerland
[i] Also at Departament de Fisica de la Universitat Autonoma de Barcelona, Barcelona; Spain
[j] Also at Department of Financial and Management Engineering, University of the Aegean, Chios; Greece
[k] Also at Department of Physics, California State University, Sacramento; United States of America
[l] Also at Department of Physics, King's College London, London; United Kingdom
[m] Also at Department of Physics, Stanford University, Stanford CA; United States of America
[n] Also at Department of Physics, Stellenbosch University; South Africa
[o] Also at Department of Physics, University of Fribourg, Fribourg; Switzerland
[p] Also at Department of Physics, University of Thessaly; Greece
[q] Also at Department of Physics, Westmont College, Santa Barbara; United States of America
[r] Also at Faculty of Physics, Sofia University, 'St. Kliment Ohridski', Sofia; Bulgaria
[s] Also at Hellenic Open University, Patras; Greece
[t] Also at Institucio Catalana de Recerca i Estudis Avancats, ICREA, Barcelona; Spain
[u] Also at Institut für Experimentalphysik, Universität Hamburg, Hamburg; Germany
[v] Also at Institute for Nuclear Research and Nuclear Energy (INRNE) of the Bulgarian Academy of Sciences, Sofia; Bulgaria
[w] Also at Institute of Applied Physics, Mohammed VI Polytechnic University, Ben Guerir; Morocco
[x] Also at Institute of Particle Physics (IPP); Canada
[y] Also at Institute of Physics and Technology, Mongolian Academy of Sciences, Ulaanbaatar; Mongolia
[z] Also at Institute of Physics, Azerbaijan Academy of Sciences, Baku; Azerbaijan

JHEP11(2024)047

[aa] *Also at Institute of Theoretical Physics, Ilia State University, Tbilisi; Georgia*
[ab] *Also at Lawrence Livermore National Laboratory, Livermore; United States of America*
[ac] *Also at National Institute of Physics, University of the Philippines Diliman (Philippines); Philippines*
[ad] *Also at Technical University of Munich, Munich; Germany*
[ae] *Also at The Collaborative Innovation Center of Quantum Matter (CICQM), Beijing; China*
[af] *Also at TRIUMF, Vancouver BC; Canada*
[ag] *Also at Università di Napoli Parthenope, Napoli; Italy*
[ah] *Also at University of Colorado Boulder, Department of Physics, Colorado; United States of America*
[ai] *Also at Washington College, Chestertown, MD; United States of America*
[aj] *Also at Yeditepe University, Physics Department, Istanbul; Türkiye*
[*] *Deceased*

JHEP11(2024)047